

## Geological Society of America Bulletin

### Composition and age of the East Antarctic Shield in eastern Wilkes Land determined by proxy from Oligocene-Pleistocene glaciomarine sediment and Beacon Supergroup sandstones, Antarctica

John W. Goodge and C. Mark Fanning

*Geological Society of America Bulletin* published online 29 March 2010;  
doi: 10.1130/B30079.1

---

#### Email alerting services

click [www.gsapubs.org/cgi/alerts](http://www.gsapubs.org/cgi/alerts) to receive free e-mail alerts when new articles cite this article

#### Subscribe

click [www.gsapubs.org/subscriptions/](http://www.gsapubs.org/subscriptions/) to subscribe to Geological Society of America Bulletin

#### Permission request

click <http://www.geosociety.org/pubs/copyrt.htm#gsa> to contact GSA

Copyright not claimed on content prepared wholly by U.S. government employees within scope of their employment. Individual scientists are hereby granted permission, without fees or further requests to GSA, to use a single figure, a single table, and/or a brief paragraph of text in subsequent works and to make unlimited copies of items in GSA's journals for noncommercial use in classrooms to further education and science. This file may not be posted to any Web site, but authors may post the abstracts only of their articles on their own or their organization's Web site providing the posting includes a reference to the article's full citation. GSA provides this and other forums for the presentation of diverse opinions and positions by scientists worldwide, regardless of their race, citizenship, gender, religion, or political viewpoint. Opinions presented in this publication do not reflect official positions of the Society.

---

#### Notes

---

Advance online articles have been peer reviewed and accepted for publication but have not yet appeared in the paper journal (edited, typeset versions may be posted when available prior to final publication). Advance online articles are citable and establish publication priority; they are indexed by PubMed from initial publication. Citations to Advance online articles must include the digital object identifier (DOIs) and date of initial publication.

---



# Composition and age of the East Antarctic Shield in eastern Wilkes Land determined by proxy from Oligocene-Pleistocene glaciomarine sediment and Beacon Supergroup sandstones, Antarctica

John W. Goodge<sup>1,†</sup> and C. Mark Fanning<sup>2,†</sup>

<sup>1</sup>*Department of Geological Sciences, University of Minnesota, Duluth, Minnesota 55812, USA*

<sup>2</sup>*Research School of Earth Sciences, Australian National University, Mills Road, Canberra, ACT 0200, Australia*

## ABSTRACT

The Precambrian East Antarctic Shield played a central role in the tectonic evolution of Rodinia and Gondwana, as well as growth of the East Antarctic Ice Sheet, yet little is known about its ice-covered interior. Glaciogenic deposits of Oligocene-Miocene and Pleistocene age on the Wilkes Land margin include glaciomarine diamictites containing basement rock clasts and fine-grained siliciclastic detritus, which provide proxy samples of the continental basement. Rock clasts obtained by dredge (81% metamorphic, 14% igneous, and 5% sedimentary lithologies) provide petrographic, geochemical, and age information about the glacial source area. Igneous clasts with Ross orogen U-Pb zircon ages (ca. 500 Ma) include a notably old ca. 585 Ma granitoid; they and Ross-age metamorphic rocks give discrete inherited-zircon age populations of 670–780, 900–1300, 1740–2300, and >2700 Ma that reflect basement sources. Paleoproterozoic rock clasts (granitoid, charnockite gneiss, and granulite gneiss) range from ca. 1720 to 1740 Ma. Detrital zircon populations from glaciomarine sediments vary with depositional age but show common terrigenous provenance ages of 460–660, 1045–1315, 1545–1815, and 2420–2605 Ma, which overlap those from inherited zircons in the Ross granitoids. Detrital zircon ages from onshore Permian and Triassic terrestrial sedimentary rocks reveal a different provenance and indicate that the glaciogenic deposits do not contain significant second-cycle material from older interior basins. Together, these data suggest that metamorphic rock units with distinctive Neoproterozoic, Paleoproterozoic, and Archean ages domi-

nate East Antarctic Shield basement inland from the eastern Wilkes Land margin, and that Ross-age granitoids either intruded or were derived by partial melting of this composite metamorphic basement.

## INTRODUCTION

The East Antarctic Shield is one of Earth's largest cratonic assemblies, and it contains rocks with a long-lived Archean and Proterozoic history (Tingey, 1991; Fitzsimons, 2000; Harley and Kelly, 2007). It is a central piece in the East Gondwana mosaic (Fig. 1; Fitzsimons, 2000), and it played an important role in the Neoproterozoic amalgamation of the Rodinia supercontinent (Goodge et al., 2008). The thickness and geothermal properties of this shield played a role in initiation of the overlying East Antarctic Ice Sheet and today affects its stability (DeConto and Pollard, 2003). A clear understanding of the geological evolution of the East Antarctic Shield therefore can provide an essential foundation for studying early crustal evolution, as well as subsequent paleogeography, resource distribution, biosphere evolution, and glacial and climate history. The history of the composite East Antarctic Shield, known from fragmentary evidence along coastal outcrops (Fig. 1), is thought to be episodic in nature. However, because of its thick cover of ice, very limited exposure, continental scale, and extreme challenge in obtaining subice samples, little is known about the composition and structure of its interior. This Precambrian shield therefore remains the most inaccessible and unexplored continental region on Earth.

A variety of methods can be used to remotely examine the ice-covered Precambrian shield of East Antarctica, including over-ice potential-field geophysics and subice drilling. However, these approaches are costly and logistically difficult. In this study, we use the provenance of glaciogenic and terrestrial sediments deposited on the

eastern Wilkes Land margin to characterize the lithology and age of ice-covered basement in this sector of Antarctica. We focused on the Adélie coast region of Wilkes Land in order to avoid possible overprinting on crustal materials by the early Paleozoic (ca. 500 Ma) Ross orogeny. Paleo-ice-flow directions for Last Glacial Maximum (LGM) ice streams and paleocurrent directions for Mesozoic river systems allow us to use sediment provenance characteristics from Neogene to latest Pleistocene glaciomarine deposits and Permian-Jurassic terrestrial sediments, respectively, as a proxy for ice-covered basement of the interior (Fig. 2). Present-day ice divides and ice-flow directions indicate that glaciogenic deposits likely have a sedimentary source in the Terre Adélie craton, and they may provide new information about the boundary between the craton and an early Paleozoic fold belt to the east.

In this paper, we present new petrographic, geochemical, and sensitive high-resolution ion microprobe (SHRIMP) U-Pb age data from lithic clasts and detrital zircons obtained from latest Pleistocene marine diamictites, Miocene marine siliciclastic deposits, and Permian-Jurassic terrestrial sedimentary rocks in order to document a secular record of sediment source variation. On the Terre Adélie margin of Wilkes Land, transported rock clasts and sediment can be used for petrographic study, geochemical analysis, clast geochronology, and detrital zircon geochronology. Together, the integration of data from petrologically distinctive lithic clasts and large detrital zircon populations from glaciomarine diamictites provides a good first-order representation of the lithic character and age of East Antarctic Shield terrains underlying the adjacent ice sheet. We compare our results with those from on-land glacial moraines (Peucat et al., 2002) and the known coastal geology of Terre Adélie and South Australia in order to provide a more complete picture of the ice-covered basement in eastern Wilkes Land.

<sup>†</sup>E-mails: [jgoodge@d.umn.edu](mailto:jgoodge@d.umn.edu); [Mark.Fanning@anu.edu.au](mailto:Mark.Fanning@anu.edu.au)

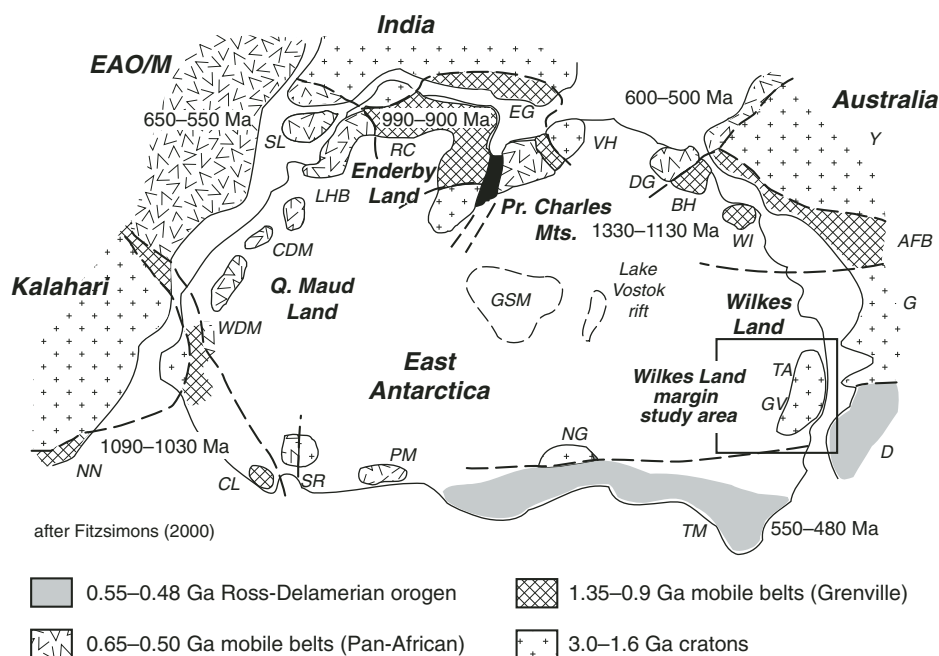


**Figure 1. Reconstruction of the major East Gondwana crustal elements in East Antarctica, southern Australia, India, and southern Africa at ca. 500 Ma (modified after Fitzsimons, 2000).** Location of study area in Wilkes Land is shown by box. Abbreviations: AFB—Albany-Fraser belt; BH—Bunger Hills; CDM—central Dronning Maud Land; CL—Coats Land; D—Delamerian orogen; DG—Denman Glacier; EAO/M—East African orogen/Mozambique belt; EG—Eastern Ghats; G—Gawler craton; GSM—Gamburtsev Subglacial Mountains; GV—George V coast; LHB—Lutzow-Holm Bay; NG—Nimrod Group; NN—Namaqua-Natal; PM—Pensacola Mountains; RC—Rayner Complex; SL—Sri Lanka; SR—Shackleton Range; TA—Terre Adélie; TM—Transantarctic Mountains; VH—Vestfold Hills; WDM—western Dronning Maud Land; WI—Windmill Island; Y—Yilgarn craton.

### PRECAMBRIAN GEOLOGY OF THE EASTERN WILKES LAND MARGIN

Outcrops of the eastern Wilkes Land margin along the George V coast and Terre Adélie consist mainly of Neoproterozoic and Paleoproterozoic high-grade gneisses and metaigneous rocks (Fig. 3; Peucat et al., 1999; Oliver and Fanning, 1997, 2002; Ménot et al., 2005; Gapais et al., 2008). The western region between Port Martin and the Dibble Ice Tongue is underlain by high-temperature, low-pressure (750 °C; 4–6 kbar) siliciclastic metasedimentary rocks with zircon U-Pb metamorphic ages of ca. 1.69 Ga (Oliver and Fanning, 1997; Peucat et al., 1999). Isolated outcrops contain ca. 1.65 Ga migmatites and ca. 1.60 Ga granitoids (Duclaux et al., 2007). The Port Martin shear zone separates these Paleoproterozoic metamorphic and igneous units from Neoproterozoic rocks exposed in the vicinity of Cape Denison. There, Archean rock units consist of heterogeneous paragneisses and granitoids, including felsic granulites, amphibolites, orthogneisses, marbles, and quartzites. U-Pb zircon ages of 2.50–2.42 Ga date metamorphism

under conditions of ~9 kbar and 800 °C (Ménot et al., 1999). These Archean rocks extend eastward to Mertz Glacier, which is thought to overlie a shear zone forming their eastern boundary (Talarico and Kleinschmidt, 2003). Shear zones farther west juxtaposed the Archean and Paleoproterozoic blocks at ca. 1.7 Ga (Duclaux et al., 2008). Granitoids with U-Pb zircon ages of ca. 500 Ma are exposed east of Mertz Glacier, but their contact relation with older basement is uncertain. The <sup>40</sup>Ar/<sup>39</sup>Ar mineral cooling ages from mylonitic rocks of the Mertz shear zone indicate that the structure underlying Mertz Glacier is older than ca. 1.5 Ga and thus is not related to the Ross orogen (Di Vincenzo et al., 2007). Outcrops of Beacon Supergroup, cut by sills of Ferrar dolerite, occur east of Ninnis Glacier at Horn Bluff, but to our knowledge, no samples of these strata are available from existing collections. In general, this assemblage of Neoproterozoic and Paleoproterozoic terrains, herein referred to as the Terre Adélie craton (TAC; Ménot et al., 1999), corresponds to geologic units in the Gawler craton of South Australia (Oliver and Fanning, 1997, 2002).

### FLUVIAL- AND GLACIAL-MARINE RECORD

The Wilkes Land continental margin formed during Gondwana breakup and separation from southern Australia ca. 85 Ma (Cande and Mutter, 1982; Müller et al., 2000). Seismic-reflection data across this sector of the Antarctic margin show that the ~100-km-wide continental shelf is underlain by faulted Early Cretaceous sedimentary basement overlain unconformably by a seaward-dipping Cretaceous to Miocene fluvial-marine succession (Hayes and Frakes, 1975; Hampton et al., 1987; Eitrem et al., 1995; Anderson, 1999); the latter includes continental-rise turbidites, among them Pliocene-Pleistocene deposits with glacial sources. The upper part of the fluvial-marine succession is overlain by subglacial and glacial-marine deposits resting on a late Eocene or early Oligocene unconformity surface that marks the onset of glaciation on the Wilkes Land shelf. Growth of the East Antarctic Ice Sheet was initiated ca. 34 Ma (Hambrey and Barrett, 1993; Zachos et al., 1996), although there is continuing controversy about stability of the ice sheet through the Neogene (Hambrey et al., 2003). The glacial-marine deposits show repeated waxing and waning of the Antarctic ice sheet to produce unconformity-bounded cycles of glaciogenic material. The present-day shelf morphology (Fig. 3) shows high-standing flat-topped banks and deep linear troughs (>1000 m), the latter of which are interpreted as scour features formed by ice streams during LGM advance (McMullen et al., 2006). The Wilkes Land margin is capped by Pleistocene glacial-marine deposits, composed of massive to stratified diamictons (Andrews and Matsch, 1983) and overlying diatomaceous mud and ooze (Domack, 1982; Leventer et al., 2006). Overcompacted sediments at the shelf break and moraines on submerged banks indicate that glacial ice expanded across the shelf during the LGM (Domack, 1982; Beaman and Harris, 2003; McMullen et al., 2006). As shown in Figure 3, sedimentological data and seafloor morphology indicate that LGM ice flow onto the shelf was focused in glaciers along the axes of the major troughs subparallel to the continental margin, whereas modern ice flow is generally radial out to the ice-sheet margin. Sedimentary lithofacies and provenance data indicate that the latest Pleistocene glacial deposits have a continental basement provenance (Domack, 1982).

For this study, we obtained samples of latest Pleistocene glaciogenic deposits, Miocene marine deposits, and Permian-Triassic terrestrial siliciclastic units from existing dredge hauls, sediment cores, and rock collections (Figs. 2B and 3). Pleistocene glaciogenic deposits on the continental margin of the George V and Adélie

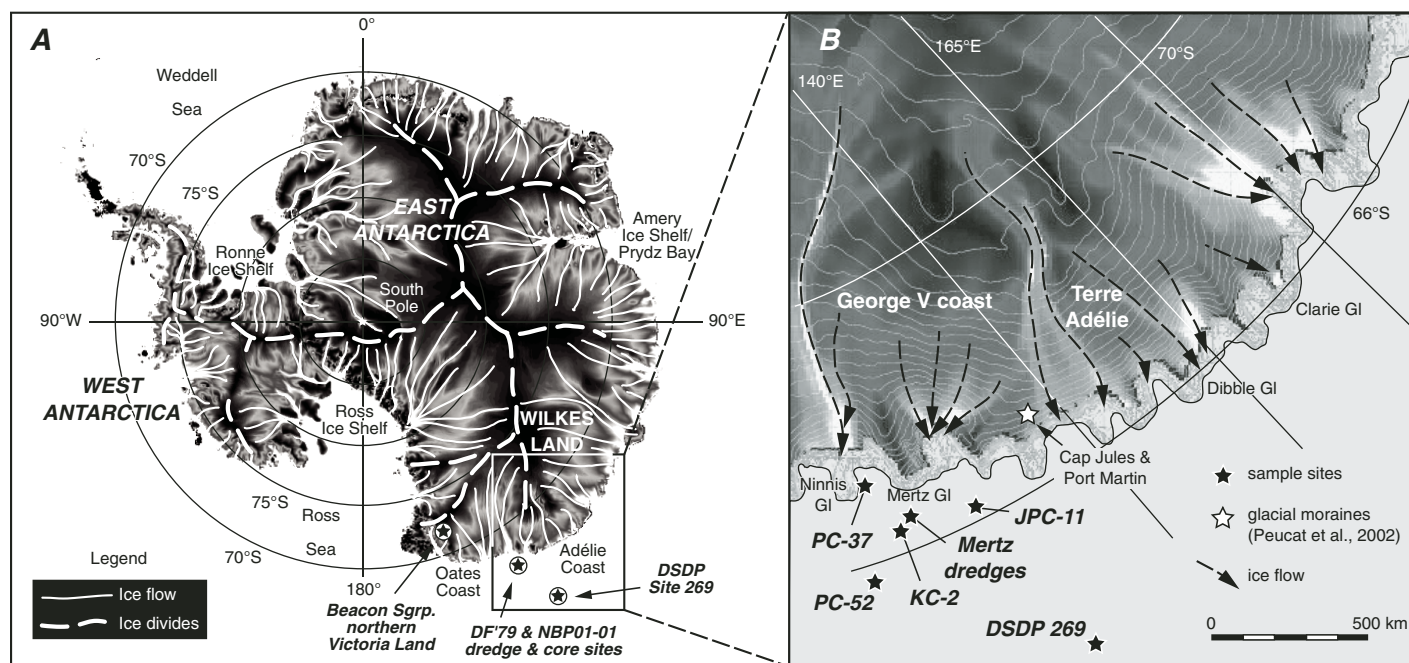


**Figure 2.** Modern ice flow in Antarctica. (A) Ice velocity field in Antarctica showing major ice-flow directions and ice divides (Barker et al., 1998). Sample sites for offshore glaciomarine deposits on the Wilkes Land margin are indicated by stars, obtained by core and dredge during cruises of the Deep Sea Drilling Project (DSDP Leg 28, 1973), U.S. Coast Guard Cutter *Glacier* (Deep Freeze, 1979), and R/V *Nathaniel B. Palmer* (Leventer et al., 2001). Also shown is location of Beacon Supergroup sampled in northern Victoria Land. Oligocene to Pleistocene ice flow is thought to be similar to the modern, so glaciogenic deposits from the Wilkes Land margin sample basement from  $\geq 750,000$  km<sup>2</sup> of the East Antarctic Shield inboard from the George V and Terre Adélie coasts. (B) Ice velocity field along the George V coast and Terre Adélie margin of Wilkes Land derived from altimetric topography (Peucat et al., 2002), with locations of sediment core and dredge sites. Brighter grayscale shading indicates faster ice velocity; gray contours show elevation of the ice surface.

coasts, including surface dredge hauls of rock clasts and piston cores of muddy diamictons with sandy intervals, were sampled during cruises of the U.S. Coast Guard Cutter *Glacier* (Operation Deep Freeze 1979; Domack, 1982) and the research vessel/icebreaker (RV/IB) *Nathaniel B. Palmer* (NBP01-01; Leventer et al., 2006). Miocene marine turbiditic sandstones were subsampled from drill cores obtained by the D/V *Glomar Challenger* during Leg 28 of the Deep Sea Drilling Project (Hayes and Frakes, 1975). Last, we obtained samples of Permian and Triassic sandstone of the Beacon Supergroup collected in northern Victoria Land (Collinson et al., 1986). Because Antarctic glaciation was initiated ca. 34 Ma, cores of Miocene and younger deposits penetrate the glacial-stage marine record. These glacial-marine sediments should yield well-mixed clast and detrital ages that can be correlated to the adjacent margin.

## CLASTS

From a shipboard dredge collection of 1359 individual pebble- to cobble-sized clasts from NBP01-01 (Schrum et al., 2004), we selected 49 representative clasts from 18 differ-

ent lithotypes identified (Table 1). We selected clasts for further study on the basis of petrologic variety and a size suitable for thin section, geochemical, and/or geochronological analysis. Thin sections from all of the clasts permitted reliable mineral and rock identification. Proportions of different clast types are summarized in Figure 4, which reflects the actual proportions of the different lithotypes in the original dredge collections rather than the unrepresentative proportions taken from our study sample subset. Of the entire diamicton clast population, we estimate that 75% of clasts are low-grade metasedimentary rocks (phyllites and psammites), up to 6% are orthogneisses and other metamorphic rock types, while unmetamorphosed igneous and sedimentary rocks make up 14% and 5%, respectively. Among igneous rocks, there is about a 13:1 ratio of granitoid to mafic (doleritic) lithologies. The metamorphic clasts are dominated by low-grade phyllites and psammites, the latter commonly preserving original detrital textures. Minor metamorphic clasts include granite gneiss, granulite gneiss, charnockite gneiss, quartzite, and schist. Most of the sedimentary clasts are relatively mature arenites, with minor graywacke. From the clast

population, low-grade siliceous metasedimentary rocks, coupled with a heterogeneous mixture of igneous and high-grade metaigneous rock types, dominate the glacial provenance on the Wilkes Land margin.

Whole-rock major-element geochemical analyses were determined by X-ray fluorescence (XRF) for six igneous and metaigneous clasts of sufficient size. All samples have subalkaline geochemical compositions and can be divided into three groups (Table 2). Two samples of granite (1-6B and 1-6D) show calc-alkalic to calcic geochemistry and trace-element affinities with Cordilleran-type volcanic-arc granites (Figs. 5A-5D), and they are typical of Ross orogen granitoids. Three dolerite or diabase samples (1-2, 1-7H, and 3-1) have mafic to intermediate composition ( $\text{SiO}_2 = 54\text{--}58$  wt%) that show tholeiitic fractionation trends (Fig. 5A). One of these (1-2) has relatively high MgO (9.85 wt%), along with high Cr and Ni, and lower large ion lithophile elements (Ba and Sr). In general, these mafic rocks have many trace-element characteristics in common with Ferrar magmas in Victoria Land (Figs. 5E-5F; Gunn, 1962, 2006), although our samples contain systematically higher Y values. It is likely these clasts are from proximal

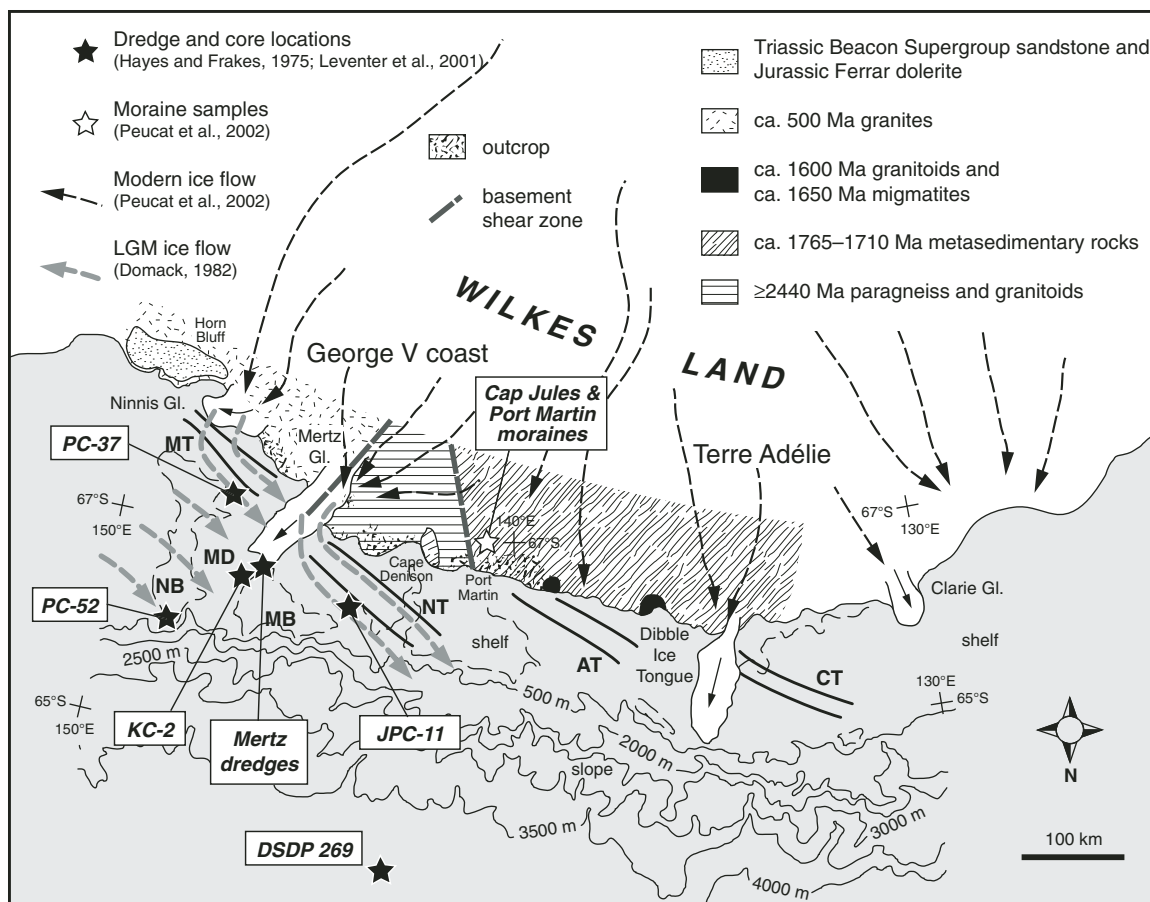


**Figure 3.** Map of George V coast and Terre Adélie region, showing principal basement rock exposures and glacial features. Precambrian igneous and metamorphic basement rocks are exposed chiefly in area between Ninnis Glacier and Dibble Ice Tongue (Oliver and Fanning 1997, 2002; Duclaux et al., 2007); Mesozoic sedimentary and igneous rocks are exposed at Horn Bluff (Mawson, 1942; Domack, 1982); recent glacial moraines were studied at Cap Jules and Port Martin (Peucat et al., 2002). Offshore bathymetry shows edge of continental shelf at ~500 m depth, corresponding to maximum extent of Neogene grounded ice, and base of continental slope at ~3500 m depth (from Anderson, 1999). Wilkes Land continental shelf morphology is marked by terminal moraines and deep troughs scoured by Last Glacial Maximum (LGM) ice streams (Domack, 1982): AT—Adélie Trough; CT—Clarie Trough; MB—Mertz Bank; MD—Mertz Depression; MT—Mertz Trough; NB—Ninnis Bank; NT—Ninnis Trough. Modern ice-flow directions (black dashed lines) are from Peucat et al. (2002), and simplified LGM flow directions (gray dashed lines) are from sedimentary petrography by Domack (1982). Variations in age of deposition or glacial transport direction might manifest in different apparent sediment provenance for individual samples as obtained from detrital zircon analysis. Dredge and core sites from NBP01–01 in Mertz Glacier area (JPC-11, KC-2, and Mertz dredges) are from Leventer et al. (2006). Piston-core sites PC-37 and PC-52 are from Deep Freeze 1979 (Anderson, 1999). Deep Sea Drilling Project (DSDP) Site 269 location is from Hayes and Frakes (1975).

Jurassic dolerite sills such as those exposed at Horn Bluff. One granulite gneiss clast (sample 3–8A) has a mafic tholeiite geochemical composition, but its origin is unclear.

### SHRIMP U-Pb GEOCHRONOLOGY

In order to ascertain the ages of basement geologic units covered by the Wilkes Land ice cap, we conducted a U-Pb zircon age study of individual rock clasts recovered from Pleistocene glaciomarine diamictos during NBP01–01,

as well as detrital zircon populations in sedimentary deposits ranging from Permian to latest Pleistocene age. Dating igneous and metamorphic clasts from the diamictos allows us to define the ages of specific lithic types, whereas the detrital zircon age populations provide a means of surveying the diversity of all provenance inputs to the continental margin. Because the U-Pb system in zircon is generally resistant to isotopic modification during erosion, weathering, and sediment transport, it provides the best estimate of basement provenance age.

### Methods

Zircon grains were separated from bulk rock and sediment samples using standard crushing, washing, heavy liquid, and paramagnetic procedures. For the provenance samples, the zircon-rich heavy mineral concentrates were poured onto double-sided tape, mounted in epoxy together with chips of the reference zircons (FC1 and SL13), sectioned approximately in half, and polished. For the geochronology samples, hand-selected zircon

TABLE 1. SUMMARY OF GLACIAL-MARINE ROCK CLASTS OBTAINED BY DREDGE, NBP01-01, WILKES LAND MARGIN, ANTARCTICA

Sample	Class*	Rock name <sup>†</sup>	U-Pb age (Ma, with error)
<b>Dredge #1</b>			
1.1A	M	Ms-Bt quartzite	
1.2	I	Bt-Cpx dolerite	
1.3	S	Feldspathic quartz arenite	
1.4	S	Arkosic litharenite	
1.5A	M	Ms-Bt schist	
1.5B	M	Chl-Ms phyllite	
1.5C	M	Bt-Chl-Ms phyllite	
1.6A	I	Ms-Bt granite	508 ± 5
1.6B	I	Bt granite	510 ± 5
1.6C	I	Bt-Ms granite	
1.6D	I	Ms-Bt granite	516 ± 6
1.6E	I	Ms-Bt granite	
1.7A	M	Ms-Bt psammite	
1.7B	M	Bt-Grt granulite	
1.7C	M	Ms-Bt psammite	
1.7D	M	Ms-Bt granite gneiss	519 ± 6
1.7E	M	Ms-Bt psammite	
1.7F	M	Ms-Bt gneiss	558–1293 <sup>§</sup>
1.7G	M	Bt-Grt granulite	
1.7H	I	Bt-Hbl-Cpx dolerite	
1.7I	M	Ms-Bt granite gneiss	≥556
1.7J	M	Bt-Ms-Chl-Ep psammite	
1.8A	M	Bt-Grt-Opx charnockite gneiss	1741 ± 8
1.8B	M	Ms-Bt psammite	
1.8C	M	Bt psammite	
1.8D	M	Ms-Bt psammite	
1.8E	S	Bt-Ms graywacke	
1.8F	I	Leucocratic Ms-Bt microgranite	584 ± 13
1.8G	M	Ms-Ep-Bt psammite	
<b>Dredge #2</b>			
2.1A	M	Ms-Bt gneiss	582–2018 <sup>§</sup>
2.1B	S	Ms feldspathic arenite	
<b>Dredge #3</b>			
3.1	I	Hbl-Bt-Cpx micrographic diabase	
3.2	M	Ms-Bt phyllite	
3.3A	I	Ms-Bt granite	506 ± 6
3.3B	I	Ms-Bt granite	484–2996 <sup>§</sup>
3.3C	I	Ms-Bt granite	
3.4	I	Bt-Hbl monzodiorite	1725 ± 9
3.5A	M	Hbl-Bt gneiss	
3.5B	M	Spotted Bt phyllite	
3.6	M	Bt-Ms quartzite	
3.7A	M	Ms-Bt psammite	
3.7B	M	Bt psammite	
3.7C	M	Ms-Bt gneiss	481–2860 <sup>§</sup>
3.7D	M	Bt psammite	
3.8A	M	Grt-Hbl-Cpx granulite gneiss	1722 ± 10
3.8B	M	Chl-Bt spotted phyllite	
3.8C	M	Ep-Chl-Ms-Bt psammite	
3.8D	M	Ep-Ms-Bt psammite	
KC-02	S	Qtz arenite	

\*I—igneous; M—metamorphic; S—sedimentary.

<sup>†</sup>Mineral abbreviations: Bt—biotite; Chl—chlorite; Cpx—clinopyroxene; Ep—epidote; Grt—garnet; Hbl—hornblende; Ms—muscovite; Opx—orthopyroxene; Qtz—quartz.

<sup>§</sup>Range indicates range of multiple grains (xenocrystic or relict detrital).

geochronology samples, each analysis consists of six scans through the mass range, with the FC-1 U-Pb reference grains analyzed for every three unknown analyses. Data were reduced using the SQUID Excel Macro of Ludwig (2001).

The U/Pb ratios were normalized relative to a value of 0.01859 for the FC-1 reference zircon, equivalent to an age of 1099 Ma (see Paces and Miller, 1993). Uncertainties given for individual analyses (ratios and ages) are at the 1 $\sigma$  level. Tera and Wasserburg (1972) concordia plots, probability density plots with stacked histograms, and weighted-mean <sup>206</sup>Pb/<sup>238</sup>U or <sup>207</sup>Pb/<sup>206</sup>Pb age calculations were carried out using ISOPLOT/EX (Ludwig, 2003). The “Mixture Modeling” algorithm of Sambridge and Compston (1994), via ISOPLOT/EX, was used for the complex data sets to deconvolve statistical age populations or groupings; from these groups, weighted-mean <sup>206</sup>Pb/<sup>238</sup>U ages were calculated, and the uncertainties are reported as 95% confidence limits.

## IGNEOUS AND METAMORPHIC CLAST AGES

Fourteen igneous and metamorphic rock clasts were selected for U-Pb geochronology in order to determine the age range of the clast population, to assess inheritance in igneous rocks, and where possible to determine the ages of multiple metamorphic events. Given that many of the clasts are of small size (order of centimeters), our selection of samples was somewhat restricted and may not be fully representative of the lithologies that were glacially transported to the Wilkes margin from the interior. Of the clasts analyzed, eight are igneous rocks and six show mineralogical and/or textural evidence of metamorphism. Given that these clast samples are out of their geological context, our approach was to analyze a relatively small number of individual zircons in each sample in order to provide the broadest possible coverage while sacrificing some age precision; nonetheless, even with typically less than 12 spot analyses per sample, we determined a wide range of ages, and on a cobble-by-cobble basis, achieved precision on the order of  $\pm 1\%$  (at 95% confidence limit) for the dominant crystallization ages. Tera-Wasserburg and Wetherill-type concordia diagrams of the data are shown in Figures 6 and 7, and individual clast data are listed in the GSA Data Repository<sup>1</sup> (Tables DR1–DR14).

<sup>1</sup>GSA Data Repository item 2010133, Tables DR1–DR21, which list SHRIMP U-Pb age results for zircons in igneous and metamorphic clasts, and detrital zircons in glacial sediments and terrestrial sedimentary rocks, is available at <http://www.geosociety.org/pubs/ft2010.htm> or by request to [editing@geosociety.org](mailto:editing@geosociety.org).

grains were placed onto double-sided tape and cast into epoxy disks.

Reflected and transmitted light photomicrographs were prepared for all zircon grains, as were cathodoluminescence (CL) scanning electron microscope (SEM) images. The CL images were used to examine the internal structures of the sectioned grains and to ensure that the ~20- $\mu$ m-diameter SHRIMP spot was wholly within a single age component within the sectioned grains; this was usually the youngest for analysis of the detrital zircon grains.

The U-Th-Pb analyses were made by sensitive high-resolution ion microprobe (SHRIMP) analysis at the Research School of Earth Sciences, Australian National University, Canberra, Australia. The SHRIMP analytical method follows Williams (1998, and references therein). For the provenance samples, zircons were analyzed sequentially and randomly until a total of 60 or more grains for each sample was reached. Each analysis consists of four scans through the mass range, with a reference zircon analyzed for every five unknown zircon analyses. For the

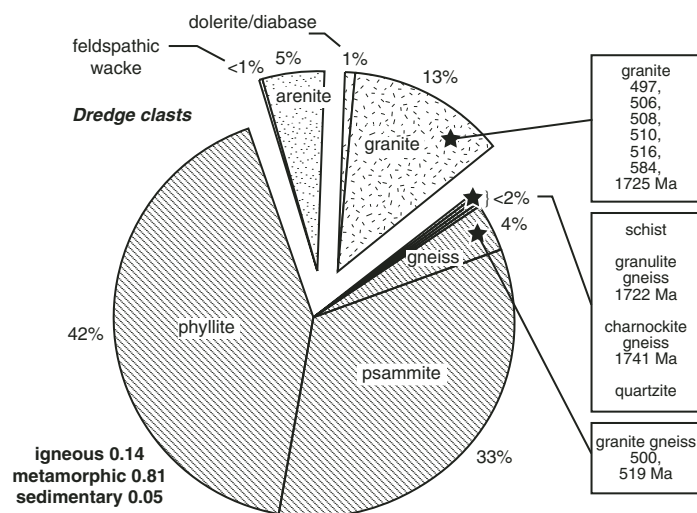


**Figure 4.** Distribution of rock types sampled by dredge on the Mertz Bank during cruise NBP01-01, from clast collection provided by E. Domack. Note that petrologic classification here is based on petrographic study and differs from that determined in hand sample by the shipboard party on NBP01-01 (Leventer et al., 2006; Schrum et al., 2004). Proportions of various lithologies reflect total clast population recovered, rather than the subsample of clasts selected for study here (Table 1). Proportions of igneous, metamorphic, and sedimentary rocks are indicated, as well as new U-Pb zircon ages for particular clast types (see Figs. 6 and 7).

**TABLE 2. GEOCHEMICAL ANALYSES OF IGNEOUS AND METAMORPHIC ROCK CLASTS, NBP01-01, WILKES LAND MARGIN, ANTARCTICA**

Sample Rock type	1-2 Dolerite	1-7H Dolerite	3-1 Diabase	1-6B Granite	1-6D Granite	3-8A Granulite gneiss
SiO <sub>2</sub>	53.74	54.40	58.07	72.73	73.14	50.66
TiO <sub>2</sub>	0.52	0.77	1.12	0.55	0.47	1.04
Al <sub>2</sub> O <sub>3</sub>	14.00	15.35	13.41	12.62	12.50	14.34
Fe <sub>2</sub> O <sub>3</sub>	9.53	11.07	12.36	4.16	3.73	12.91
MnO	0.17	0.18	0.18	0.06	0.05	0.20
MgO	9.85	4.56	3.06	1.38	0.67	6.87
CaO	9.95	9.97	7.67	1.75	1.79	10.78
Na <sub>2</sub> O	1.58	2.19	2.46	2.45	2.59	2.29
K <sub>2</sub> O	0.66	1.05	1.59	3.69	4.51	0.64
P <sub>2</sub> O <sub>5</sub>	0.08	0.12	0.17	0.13	0.13	0.09
LOI	0.00	0.18	0.16	0.42	0.13	0.48
Sum	100.05	99.83	100.24	99.97	99.70	100.30
Ba	146	235	451	696	638	175
Ce	14	25	40	57	112	14
Co	54	46	57	10	7	57
Cr	474	18	11	54	24	103
Cu	61	129	156	10	7	107
Ga	14	18	19	15	17	18
La	9	13	21	30	55	5
Nb	5	7	9	13	10	5
Ni	149	51	27	27	13	77
Pb	7	10	12	29	26	6
Rb	23	39	59	151	196	28
Sc	41	43	42	10	6	48
Sr	102	144	145	163	117	148
Th	4	5	7	13	34	3
U	3	2	3	3	3	0
V	218	238	266	66	35	324
Y	18	27	36	29	45	22
Zn	72	87	103	53	47	96
Zr	68	111	178	209	294	68
Fe*	0.49	0.71	0.80	0.75	0.85	0.65
MALI	-7.71	-6.73	-3.62	4.40	5.30	-7.85

Note: Analyses were completed at the Department of Geology, Macalester College. Results for major elements are expressed as weight percent of the oxide; trace elements are in ppm (mg/g). Values are averages of at least two analyses. Fe was analyzed as total Fe<sub>2</sub>O<sub>3</sub>. All samples were dried for 2 h at 105 °C prior to loss on ignition (LOI); LOI is reported as percent weight change of predried samples after sintering for 1 h at 1000 °C. Fe\* = (Fe<sub>tot</sub>)/(Fe<sub>tot</sub> + MgO); MALI = K<sub>2</sub>O + Na<sub>2</sub>O - CaO (Frost et al., 2001). MALI—modified alkali-lime index = K<sub>2</sub>O + Na<sub>2</sub>O - CaO (Frost et al., 2001).

## Igneous Clasts

### 1-6A, Muscovite-Biotite Granite

Sample 1-6A is a gray equigranular medium- to coarse-grained Ms-Bt granite with dark quartz and CI ~10. There is no evident solid-state mineral deformation, but it shows a weak foliation coupled with a moderate lattice preferred orientation. Zircons in this rock are generally of two types: lozenge-shaped stubby crystals with subround terminations and dark sector zonation under CL, and long slender clear prisms showing igneous zoning under CL. The dark sector-zoned cores of three grains (1, 5, 6) have <sup>206</sup>Pb/<sup>238</sup>U ages between ca. 530 and 585 Ma (Table DR-1), whereas the six slender grains form a simple bell-shaped peak of <sup>206</sup>Pb/<sup>238</sup>U ages in the range ca. 500–515, and these give a weighted-mean age of 508.3 ± 5.8 Ma (mean square of weighted deviates [MSWD] = 0.70; Fig. 6A). We interpret the older core ages as evidence of metamorphic inheritance or early igneous crystallization, and the younger ages as indicating final crystallization of the igneous rock at ca. 508 Ma.

### 1-6B, Biotite Granite

Sample 1-6B is a light-gray, coarse-grained, weakly porphyritic Bt granite with smoky quartz and CI ~5–10. It contains tabular and subhedral crystals of zoned plagioclase and traces of muscovite. There is no evident solid-state deformation fabric. Geochemically, it is a magnesian granite (Fe\* = 0.75 at 73 wt% SiO<sub>2</sub>; Fig. 5B; Table DR2) typical of evolved continental-margin Cordilleran granite suites (Frost et al., 2001), and it is borderline calcic to calc-alkaline. Zircons in this rock are generally clear, stubby, faceted prisms showing complex internal zoning in CL. Most grains show an internal domain of growth banding or sector zoning, surrounded by an outermost zoned igneous component. One grain (6) has the same internal structure as others, but the area analyzed is significantly enriched in common Pb, and the <sup>206</sup>Pb/<sup>238</sup>U age of ca. 630 Ma is not considered significant. Analyses from the zoned CL overgrowths of two grains (3 and 8; Table DR2) have <sup>206</sup>Pb/<sup>238</sup>U ages of ca. 485 Ma and ca. 480 Ma, respectively. The areas analyzed are slightly enriched in common Pb, and whereas these two overgrowths may provide an estimate for the youngest period of zircon formation, these young analyses most probably reflect radiogenic Pb loss. The remaining six analyses of wide zoned overgrowth domains have <sup>206</sup>Pb/<sup>238</sup>U ages ranging from ca. 505 to 515 Ma and are the dominant age component for this sample. We interpret the weighted-mean <sup>206</sup>Pb/<sup>238</sup>U age of 510.0 ± 5.6 Ma (MSWD = 0.74; Fig. 6B) to represent the best estimate for the age of crystallization of this granite.

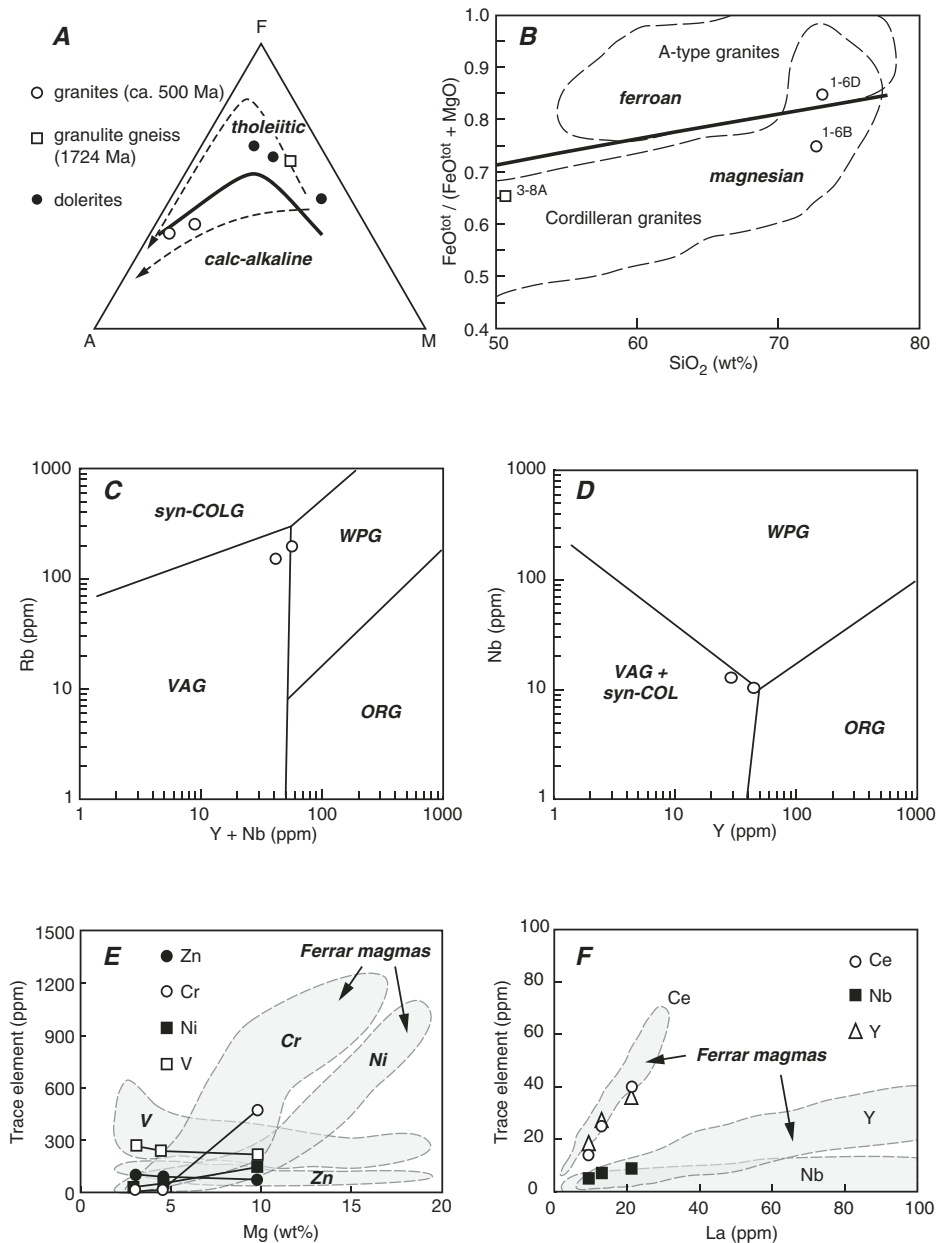


**Figure 5.** Plots of geochemical analyses for selected igneous and metamorphic clasts obtained by dredge haul from cruise NBP01-01 (Tables 1 and 2). Rocks include mafic dolerites (black circles), granites (samples 1-6B and 1-6D, white circles) with Ross orogen crystallization ages, and one granulite gneiss (sample 3-8A, white square) that has a metamorphic age of  $1724 \pm 8$  Ma. (A) AFM diagram, with division between tholeiitic and calc-alkaline compositions (Irvine and Baragar, 1971) and typical trends shown by dashed line. (B)  $\text{Fe}_2\text{O}_3^{\text{total}}/(\text{Fe}_2\text{O}_3^{\text{total}} + \text{MgO})$  versus  $\text{SiO}_2$  ( $\text{Fe}^*$ ; after Frost et al., 2001). (C) Rb versus Y + Nb, with fields for different types of granitic rocks from Pearce et al. (1984). Syn-COLG—syn-collisional granite; WPG—within-plate granite; VAG—volcanic-arc granite; ORG—orogenic granite. (D) Nb versus Y, with fields for different types of granitic rocks from Pearce et al. (1984). (E) Trace-element variations in samples of mafic rocks compared to Jurassic Ferrar dolerites in Antarctica (Gunn, 2006). (F) Rare earth elements versus La, with variations observed in Ferrar magmas (Gunn, 2006). The mafic rocks show compositions and tholeiitic trends similar to the Ferrar dolerites, whereas the ca. 500 Ma granites show calc-alkaline trends and trace-element compositions consistent with a volcanic-arc setting like that of the Andean-type Ross orogen (Allibone et al., 1993). The granulite gneiss shows a mafic tholeiitic trend and trace-element compositions consistent with an origin as a lower-crustal melt.

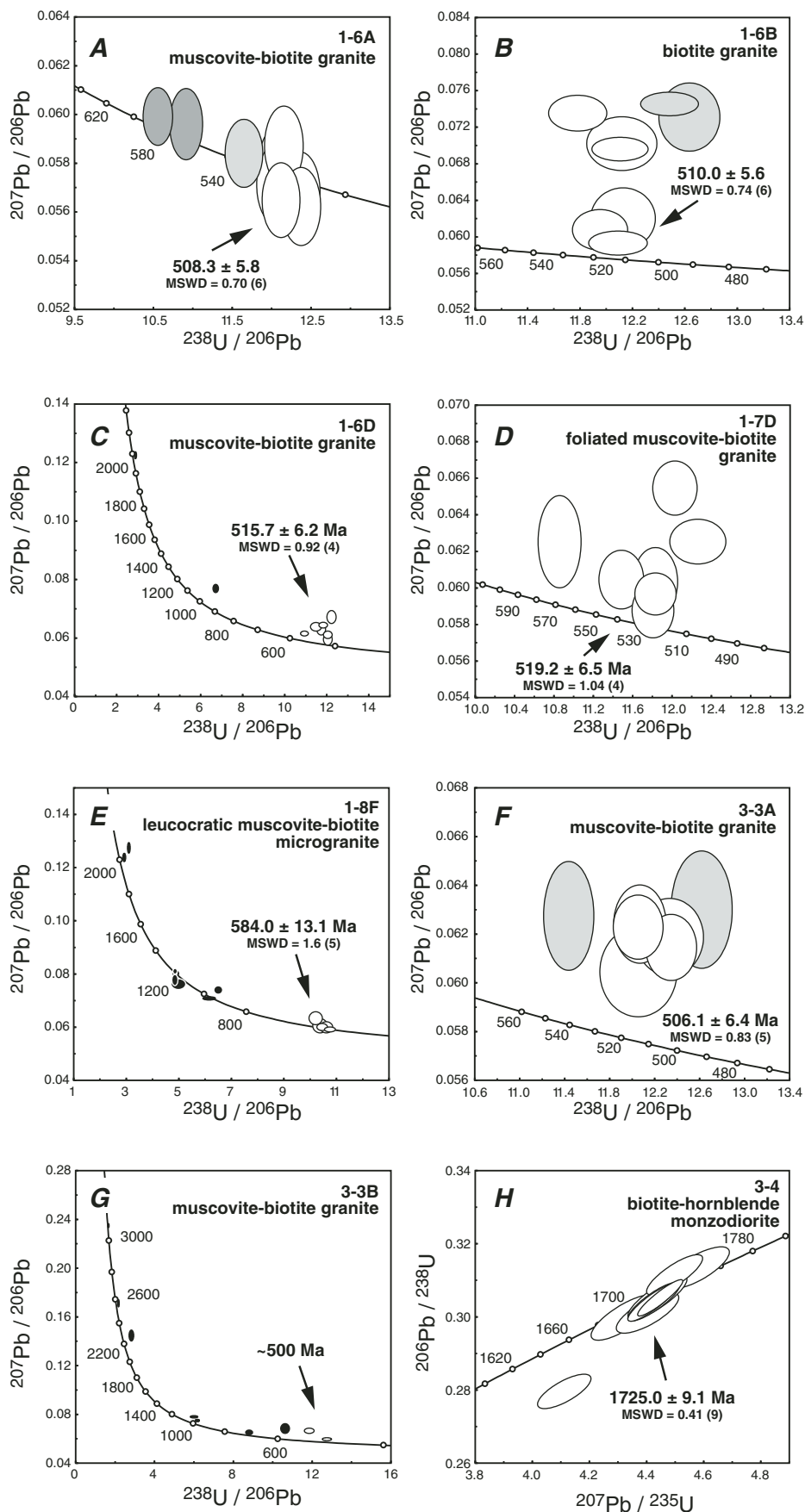
#### 1-6D, Muscovite-Biotite Granite

Sample 1-6D is a white to gray, medium-grained, equigranular Ms-Bt granite with yellow alteration and CI  $\sim 15$ . It contains tabular and subhedral crystals of plagioclase, and it shows no evident solid-state deformation fabric. Geochemically, it is a ferroan granite ( $\text{Fe}^* = 0.85$  at 73 wt%  $\text{SiO}_2$ ; Fig. 5B; Table 2) typical of continental-margin Cordilleran granite suites (Frost et al., 2001), and it is calc-alkaline as defined by its alkali-lime index. Zircons in this granite are heterogeneous and have a wide range of morphologies, including dark, rounded, zoned grains, doubly terminated stubby crystals, and relatively clear prisms. Most grains show a prominent core under CL imaging, with variably thick but banded external overgrowths. Of nine grains analyzed, five are of older inherited components (Fig. 6C). Analysis of the core to grain 1 is  $\sim 5\%$  discordant with a  $^{207}\text{Pb}/^{206}\text{Pb}$  age of ca. 1985 Ma (Table DR-3), whereas the analysis of grain 9 is poorly sited, of a mixed core and rim area, yielding  $\sim 15\%$  age discordance and a  $^{207}\text{Pb}/^{206}\text{Pb}$  age of ca. 1033 Ma. Four analyses, taken from CL-dark overgrowths, have  $^{206}\text{Pb}/^{238}\text{U}$  ages ranging from ca. 500 to 520 Ma, with a weighted-mean age of  $515.7 \pm 6.2$  Ma (MSWD = 0.92). Three analyses (5, 6, 8) have somewhat older  $^{206}\text{Pb}/^{238}\text{U}$  ages ranging from ca. 530 to 560 Ma, and they are not included in the weighted-mean calculation. We interpret the age of ca. 516 Ma as the best estimate for crystallization of this granite, although the zircon population is heterogeneous, complexly structured, and clearly records the presence of older inheritance.

#### 1-7D, Foliated Muscovite-Biotite Granite

Sample 1-7D is a light to medium-gray, heterogeneous layered granite, with similar mineralogy in each of three textural zones (layers  $\geq 0.5$  cm). It displays an igneous crystallization texture, suggesting the rock is magmatic, but it also shows a weak lattice preferred orientation of quartz and feldspar. Most of the zircon grains in this sample are clear, faceted prisms, and nearly all consist of outer oscillatory-zoned igneous zircon with inherited cores showing sector-zoning or parallel growth banding. The analyses of grains 4 and 9 are significantly enriched in common Pb, have younger  $^{206}\text{Pb}/^{238}\text{U}$  ages of ca. 290 Ma and ca. 320 Ma, and are interpreted to have lost significant amounts of radiogenic Pb; these analyses are not considered further. The areas analyzed in grains 1, 7, and 12 are not texturally different than other grains analyzed, but they have distinctly older  $^{207}\text{Pb}/^{206}\text{Pb}$  ages of ca. 1725, 3160, and 2695 Ma, respectively (Table DR4). Analyses of the outermost, oscillatory-zoned

**Figure 6.** Tera-Wasserburg and Wetherill concordia age diagrams for zircons in igneous clast samples collected by dredge haul on the Wilkes Land margin by cruise NBP01-01 (Table 1). White ellipses show analyses used in determination of weighted-mean igneous crystallization ages; gray and black ellipses show other age analyses, typically of interior zircon domains. Ages and uncertainties of clustered populations were determined from weighted means, except where noted as concordia ages. MSWD—mean square of weighted deviates. Complete sensitive high-resolution ion microprobe (SHRIMP) analytical data are listed in Tables DR1–8 (see text footnote 1).



components in seven grains give  $^{206}\text{Pb}/^{238}\text{U}$  ages ranging from ca. 500 to 565 Ma (Table DR4), and the four youngest have a weighted-mean  $^{206}\text{Pb}/^{238}\text{U}$  age of  $519.2 \pm 6.5$  Ma (MSWD = 1.04; Fig. 6D). We regard the age of 519 Ma to represent the best estimate for crystallization of the granite, although textural evidence suggests that it experienced deformation during or after solidification. The moderate Th/U ratios of the youngest zircon analyses and the parallel growth banding indicate that these zircons grew from a melt rather than during metamorphism, so it is most likely that this granite was formed by synkinematic emplacement.

#### 1–8F, Leucocratic Muscovite-Biotite Microgranite

Sample 1–8F is a light-gray, fine-grained, equigranular Ms-Bt granite (CI ~3), showing granoblastic microtexture. It contains domains of neoblastic quartz subgrain formation, but no other evidence of intracrystalline deformation and no evident lattice preferred orientation. Fine-grained micas are concentrated in clumps along grain boundaries. It may have a microgranite or aplite protolith, possibly formed by in situ crustal melting. Zircons in this sample are heterogeneous in form and texture, including clear prismatic grains, strongly zoned grains, and many round to subround grains. The CL images further highlight the heterogeneous nature of this zircon population, ranging from a relatively simple homogeneous gray character to a complex structurally zoned and mottled appearance. Five grains (4, 5, 7, 9, and 10) with indistinct internal growth zonation have Neoproterozoic  $^{207}\text{Pb}/^{206}\text{Pb}$  ages of ca. 1040, 1095, 1210, 1325, and 970 Ma, respectively (Table DR5). Two grains (3 and 6) are sub-round fragments showing uniform CL response and slightly discordant  $^{207}\text{Pb}/^{206}\text{Pb}$  ages of

ca. 2060 and ca. 2015 Ma. The remaining five grains are uniform to weakly zoned and have  $^{206}\text{Pb}/^{238}\text{U}$  ages ranging from ca. 570 to 600 Ma; a weighted-mean value of these  $^{206}\text{Pb}/^{238}\text{U}$  ages is  $584.0 \pm 13.1$  Ma (MSWD = 1.6; Fig. 6E). We regard this late Neoproterozoic age as the best estimate for maximum crystallization of the microgranite. The grains giving Paleoproterozoic and Grenville-type Neoproterozoic ages are interpreted as distinct inherited zircon subpopulations in the microgranite, and the predominance of these older age components is consistent with an interpretation of in situ partial melting of a heterogeneous source material; that is, this is likely to be an S-type granitoid.

### 3–3A, *Muscovite-Biotite Granite*

Sample 3–3A is a light-green-gray, coarse-grained granite with CI ~15. It is mostly equigranular but contains slightly coarser feldspars, including compositionally zoned plagioclase. There is no evident intracrystalline deformation, except minor fractures and kinks in some coarse biotite grains, and no evident lattice preferred orientation. Zircons in this sample are of two types: small, equant faceted grains, and more elongate to slender clear prisms. The smaller equant grains typically show inherited older cores with thin, zoned igneous rims under CL, whereas the slender prisms show relatively simple parallel igneous growth zoning. Seven of the analyzed grains have  $^{206}\text{Pb}/^{238}\text{U}$  ages ranging from ca. 490 to 540 Ma (Table DR6), and five of these give a weighted-mean  $^{206}\text{Pb}/^{238}\text{U}$  age of  $506.1 \pm 6.4$  Ma (MSWD = 0.83; Fig. 6F). Two of the small equant grains (1 and 2) have Proterozoic ages of ca. 1785 and 1120 Ma, respectively. The 506 Ma age of the well-formed prisms represents the best estimate for igneous crystallization of this granite, which also contains distinctly older inherited Neoproterozoic and Paleoproterozoic zircon components.

### 3–3B, *Muscovite-Biotite Granite*

Sample 3–3B is a white to light-gray, medium-grained, equigranular Ms-Bt granite (CI ~5) with prominent dark biotite. It has a massive granitic texture with some subhedral tabular plagioclase crystals, and it shows no evident deformation fabric. Most of the zircons in this sample are relatively clear, short faceted prisms; some are semi-equant and round to subround. Their internal growth structure is variable but mostly complex; many grains have distinct cores, including oscillatory zoned, sector zoned, or homogeneous metamorphic components, surrounded by thin overgrowths. The zircons yield highly variable ages (Table DR7). Three grains (2, 4, and 8) are relatively clear faceted prisms that have old, nearly con-

cordant  $^{207}\text{Pb}/^{206}\text{Pb}$  ages of ca. 2275, 3075, and 2560 Ma, respectively. Two grains (3 and 5) have similar Neoproterozoic  $^{207}\text{Pb}/^{206}\text{Pb}$  ages of ca. 980 Ma. Four grains (1, 6, 7, and 9) have late Neoproterozoic to Cambrian ages (Fig. 6G), but these range widely from ca. 485 to 690 Ma with little overlap. Within this younger age range, the  $^{206}\text{Pb}/^{238}\text{U}$  ages for grains 7 and 9 at ca. 485 Ma and ca. 515 Ma, respectively, suggest that this granite crystallized at a maximum age of ca. 500 Ma. Although this rock displays a granitic texture and contains some relatively young igneous zircons, indicating crystallization no older than ca. 500 Ma, it clearly contains an abundance of inherited zircon with Neoproterozoic and Archean ages.

### 3–4, *Biotite-Hornblende Monzodiorite*

Sample 3–4 is a reddish-gray, fine- to medium-grained, foliated Bt-Hbl monzodiorite (CI ~20). It shows an inequigranular phaneritic texture with coarse tabular subhedral plagioclase crystals (altered). Zircons in this sample are uniformly clear prisms; some have bipyramidal terminations, but most are fragmented. Under CL, the grains have a uniform appearance and little zonation, as is common in mafic igneous zircon; some display internal igneous growth bands, and a few have possible very narrow overgrowths. We analyzed nine grains, and all have Paleoproterozoic  $^{207}\text{Pb}/^{206}\text{Pb}$  ages ranging from 1707 to 1745 Ma (Table DR8); a weighted-mean age of  $1725.0 \pm 9.1$  Ma (MSWD = 0.41; Fig. 6H) represents the best estimate for crystallization of this monzodiorite. There is no evidence for either older inheritance or younger growth.

## Metamorphic Clasts

### 1–7F, *Muscovite-Biotite Gneiss*

Sample 1–7F is a gray, medium-grained equigranular layered gneiss (layers  $\geq 2$  mm; CI ~5). It contains granoblastic quartz and feldspar interlocked with finer micas, with biotite somewhat coarser than muscovite. There is no evident intracrystalline strain and no lattice preferred orientation in this sample, yet its granoblastic and layered texture indicates it is metamorphic. Zircons in this sample vary in appearance, ranging from well-formed prisms, to faceted equant grains, fragments, and round to subround grains. Likewise, their CL appearance is highly variable, ranging from relatively simple oscillatory-zoned or bright homogeneous grains, to complexly structured grains with sector or oscillatory-zoned cores overgrown by oscillatory-zoned rims, and various combinations of all these components. For this study, the SHRIMP spot analyses focused on the outer domains of relatively clear, faceted crystals in order to re-

cover age information about the youngest zircon growth stages. Their ages range discontinuously from ca. 560 to 1300 Ma (Fig. 7A; Table DR9). Two grains (5 and 9) have  $^{206}\text{Pb}/^{238}\text{U}$  ages of ca. 560 and ca. 600 Ma, respectively; these grains are characterized by broad oscillatory bands in CL and moderate Th/U ratios indicative of igneous origin. Three grains (3, 6, and 8) have  $^{206}\text{Pb}/^{238}\text{U}$  ages of ca. 770 Ma, one of which has very low Th/U and dark indistinct zonation, possibly reflecting a metamorphic origin. The remaining grains have ages of ca. 670, 1025, 1075, and 1295 Ma. The origin of this clast is ambiguous. Although texturally a metamorphic rock and containing disparate zircon ages, its youngest zircons lack features commonly observed in metamorphic zircons and instead have characteristics of igneous zircons. We therefore interpret this rock as being largely igneous in origin, in which the majority of zircons are relict detrital or inherited grains, yet the rock shows evidence of recrystallization and/or differentiation. Given the lack of a replicate age for the youngest analysis, it is not possible to define a lower age bound for this rock, but it appears to be related to the most recent Ross-age basement activity in the region.

### 1–7I, *Muscovite-Biotite Granite Gneiss*

Sample 1–7I is a light greenish-gray, fine-grained gneiss with diffuse layers. It has a medium-grained granoblastic texture with interlocking anhedral grains of quartz and feldspar and grain boundaries pinned by micas. There is no evident intracrystalline strain or lattice preferred orientation. Zircons in this sample range from clear well-formed prisms to faceted and round equant grains. The CL images show mostly oscillatory internal zoning, but some grains are complexly structured with zoned cores and bright CL rims or intermediate growth regions. Like clast 1–7F, this sample yielded a wide range of ages (Fig. 7B). Four grains (3, 7, 8, and 9) have young  $^{206}\text{Pb}/^{238}\text{U}$  ages between ca. 555 and 585 Ma, although two of these with round shape have relatively older ages of ca. 580 and ca. 585 Ma (Table DR10). Spot ages for the two youngest grains (3 and 7) at ca. 555–560 Ma were obtained from relatively simple oscillatory-zoned outer zircon growth areas within these grains. Other grains have  $^{207}\text{Pb}/^{206}\text{Pb}$  ages of ca. 890, 910, 1065, 1205, and 3385 Ma. As with clast 1–7F, it is difficult to derive an unambiguous history from a small number of analyses, but this rock appears to have formed by largely igneous processes modified by metamorphic and deformation effects of the Ross orogeny at ca. 560 Ma. The scatter of ages probably reflects the presence of either detrital or inherited zircons in the protolith.

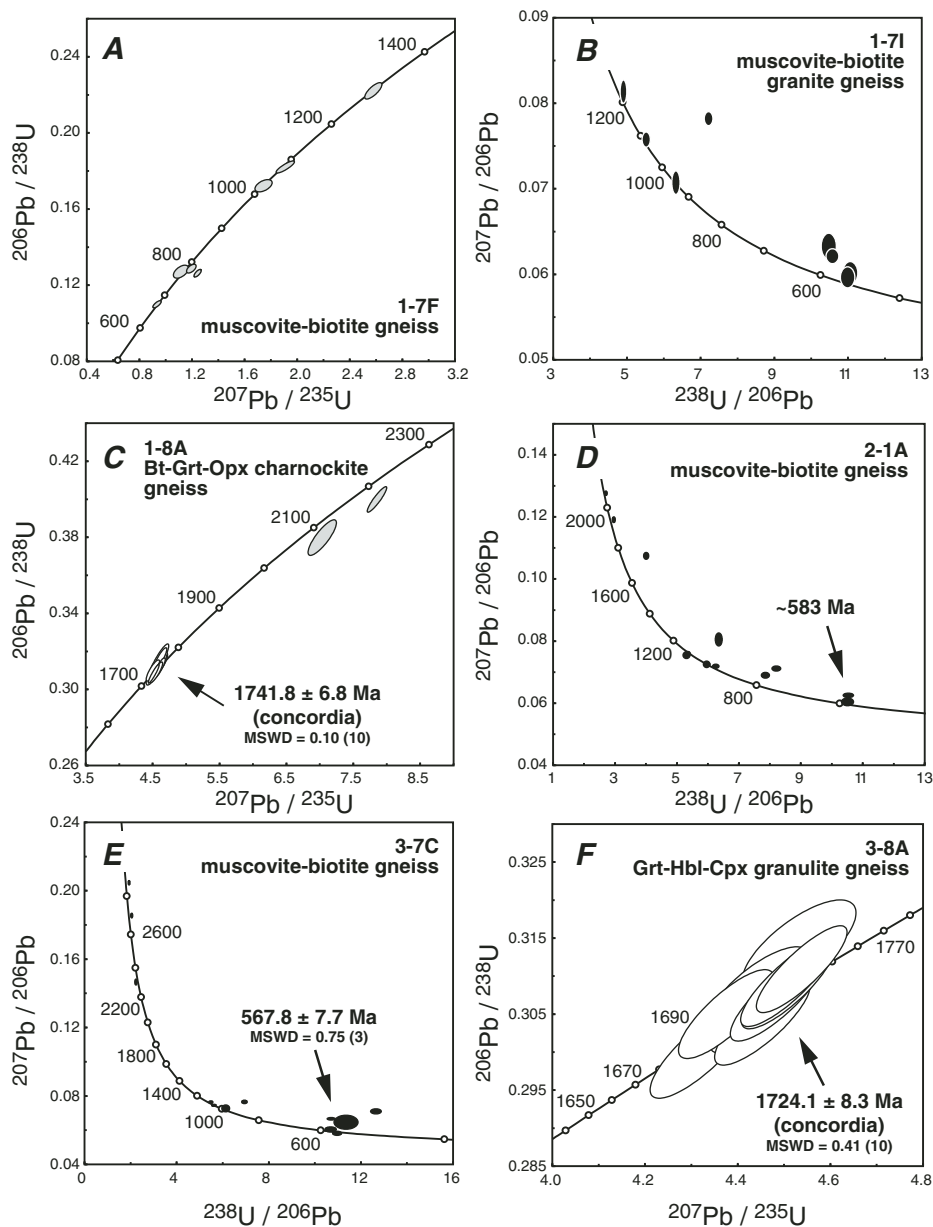


**Figure 7.** Tera-Wasserburg and Wetherill concordia age diagrams for zircons in metamorphic clast samples collected by dredge haul on the Wilkes Land margin by cruise NBP01–01 (Table 1). Ages and uncertainties of clustered populations were determined from weighted means, except where noted as concordia ages. MSWD—mean square of weighted deviates. In some cases (e.g., A, C, F), not all zircon grain ages are shown in order to emphasize the most common and/or young age range in the sample. Complete sensitive high-resolution ion microprobe (SHRIMP) analytical data are listed in Tables DR9–14 (see text footnote 1).

#### 1–8A, Biotite-Garnet-Orthopyroxene Charnockite Gneiss

Sample 1–8A is an olive-green, foliated gneiss with medium-grained porphyroblasts of garnet in a finer matrix that includes pyroxene and biotite. Its foliated texture is defined by a grain-shape preferred orientation of coarser dark garnet porphyroblasts (0.5–2.0 mm) with weakly

elongate shape and tails. A granoblastic texture of anhedral quartz and feldspar in the groundmass shows moderate quartz lattice preferred orientation but no subgrain formation. This sample probably has a sedimentary or volcanic protolith; it is texturally not a granitoid or other phaneritic igneous rock. Zircons in this sample are uniformly equant, round brown grains show-

ing prevalent fractures; a few elongated crystals show concentric internal structure. In CL, they generally show internal sector zonation or have a relatively homogeneous character; many have thin brighter CL rims. Two of the grains (4 and 11) are texturally similar to the others, but they have slightly discordant  $^{207}\text{Pb}/^{206}\text{Pb}$  ages of ~ca. 2160 and 2260 Ma, respectively (Table DR-11). The remaining 10 grains have  $^{207}\text{Pb}/^{206}\text{Pb}$  ages ranging from 1730 to 1770 Ma, with a concordia age of  $1741.8 \pm 6.8$  Ma (Fig. 7C). Although the zircons analyzed have moderate Th/U ratios, their texture, sector zonation, and associated mineral paragenesis all indicate these are metamorphic zircons. Therefore, we regard the age of 1742 Ma for this rock as reflecting a period of Paleoproterozoic high-grade metamorphism in the Wilkes Land basement.

#### 2–1A, Muscovite-Biotite Gneiss

Sample 2–1A is a light-gray, fine-grained equigranular Ms-Bt gneiss. It is weakly foliated with sparse micas in an interlocking groundmass of granoblastic quartz and feldspar; there is no evident lattice preferred orientation. The rock contains a thin vein of black tourmaline. Zircons from this gneiss are heterogeneous, ranging from elongate to equant, subhedral forms to round-subround and irregular shapes that appear metamict in places. The wide range of CL internal structures further documents the heterogeneous nature of this zircon population, suggesting that this is a detrital zircon population of mixed igneous and metamorphic types. Twelve zircon analyses give ages between ca. 580 and 2070 Ma (Fig. 7D). Two grains (1 and 11) have  $^{206}\text{Pb}/^{238}\text{U}$  ages of 584 and 582 Ma, two have ages between 740 and 770 Ma (grains 4 and 10), several have Grenville-like ages between 955 and 1115 Ma, and the remaining grains have a variety of Paleoproterozoic ages (Table DR12). Analyses for grains 1 and 11 were taken on weakly to unzoned outer areas, indicating that these ages may reflect a period of relatively young (Ross-age?) metamorphism in a paragneiss containing older detrital and/or inherited grains reflecting Paleoproterozoic and Neoproterozoic sources.

#### 3–7C, Muscovite-Biotite Gneiss

Sample 3–7C is a light-gray, fine-grained equigranular Ms-Bt gneiss showing a weakly layered (1–2 cm) and foliated texture with a peppy distribution of dark micas. It has a uniform granoblastic texture with a weak lattice preferred orientation defined by quartz. This gneiss contains a variety of zircons, including clear faceted prisms, prism sections with round tips, dark round grains, and subangular fragments. They are likewise heterogeneous in CL, showing

a range of igneous and metamorphic types. Four grains (4, 8, 9, and 10) showing relatively clear prismatic form have  $^{206}\text{Pb}/^{238}\text{U}$  ages ranging from 540 to 575 Ma (Table DR13), with three (grains 4, 9, and 10) giving a weighted-mean age of  $567.8 \pm 7.7$  Ma (MSWD = 0.75; Fig. 7E). The age of grain 3 is younger, but the area analyzed is interpreted to have lost radiogenic Pb and so is not considered as meaningful. Four grains (6, 7, 11, and 12) have Grenville-like ages ranging from ca. 985 to 1085 Ma. Three grains (1, 2, and 5) have distinctly old ages of 2695, 2860, and 2300 Ma, respectively, obtained from wide sector-zoned domains that may reflect an ancient metamorphic source terrain. Although it is difficult to distinguish an igneous from a metamorphic origin for this rock, we conclude that it experienced a period of metamorphism at ca. 568 Ma and that its protolith contains significant older material, including some grains of Late Archean age.

### 3–8A, Garnet-Hornblende-Clinopyroxene Granulite Gneiss

Sample 3–8A is a dark-brown-gray to black, fine-grained mafic gneiss showing faint compositional layering and a weak foliation, cut by white veins. Overall, it has a granoblastic texture, but it contains isolated domains of symplectite intergrowths of pyroxene, amphibole, feldspar, and opaque mineral surrounding relict garnet. Based on its mineralogy and texture, we considered that this clast represented a part of the Ross-age igneous-arc basement, but its geochemistry is notably tholeiitic, more magnesian, and less evolved than known examples of Ross-type granites (Fig. 5; Table 2). Zircons in this gneiss are uniformly small, generally equant to elongate, round to sub-round faceted grains showing internal sector zoning in CL. The ten grains analyzed yield concordant  $^{207}\text{Pb}/^{206}\text{Pb}$  ages in the range 1690–1760 Ma. All ten analyses give a concordia age of  $1724.1 \pm 8.3$  Ma (Table DR-14; Fig. 7F), which we regard as the best estimate for the age of Paleoproterozoic metamorphism in this high-grade basement granulite.

### Inherited Zircon Ages

Figure 8A shows the distribution of old ages obtained for 21 inherited zircons in six of the Ross-age granitoids discussed above (1–6B, 1–6D, 1–7D, 1–8F, 3–3A, and 3–3B). The range of ages includes groups familiar to East Gondwana: (1) 600–700 Ma, possibly reflecting Neoproterozoic rifting or Pan-African tectonism; (2) 900–1300 Ma, common in widespread Grenville-age basement; (3) 1725–2000 Ma, reflecting a period of significant

Paleoproterozoic crust production worldwide; and (4) 2700–3200 Ma, corresponding to major Archean crust generation. The age grouping at ca. 1700 Ma corresponds directly with the age obtained for monzodiorite sample 3–4. These older inherited ages help to establish the range of possible crust-formation ages in the hidden Wilkes Land basement as carried by the Ross-age granitoids, although they themselves may represent multicycle zircon. Of these age groups, however, only the Grenville-type and Paleoproterozoic ages are well represented in sedimentary detrital zircon records (discussed in the following). Notably absent from the inherited igneous zircons are ages of ca. 1400 and ca. 1600 Ma; the former ages are seen in detrital zircon populations from the central Ross orogen (Goodge et al., 2002, 2004), and the latter age represents the age of Gawler Range volcanism in the Gawler craton of South Australia (Fanning et al., 1988), as also observed in moraine clasts from Port Martin on the Adélie coast (Peucat et al., 2002). The absence of these ages in our data set suggests that our samples are derived from a segment of the ice-covered region of interior Wilkes Land that does not contain significant Mesoproterozoic crust.

Zircon analyses obtained from the metamorphic clasts include a large number of ages that predate the Ross orogen (Fig. 8B). Similar age groups are evident as compared to the inherited igneous zircons: 600–800, 900–1300, 1700–2300, and  $\geq 2600$  Ma. Two clasts with metamorphic ages of 1720–1740 Ma confirm the importance of this Paleoproterozoic age component in the local basement, whereas there are no known occurrences of 600–800 and 900–1300 Ma basement in the Terre Adélie region.

### DETRITAL ZIRCON AGES

Sediment cores collected on the Wilkes Land continental shelf and outer rise sampled glaciogenic sediment delivered from the continent (Fig. 3). Piston cores of latest Pleistocene glaciogenic diamict deposits were collected in 1979 as part of the Deep Freeze cruise by U.S. Coast Guard Cutter *Glacier* and in 2001 by cruise NBP01–01 of RV/IB *Nathaniel B. Palmer* (Anderson et al., 1979; Domack, 1982; Anderson, 1999; Leventer et al., 2006); we obtained subsamples of these cores at the Antarctic Research Facility at Florida State University. Samples of Oligocene-Miocene sediment from Site 269 of Deep Sea Drilling Project (DSDP) Leg 28 (Hayes et al., 1975; Hayes and Frakes, 1975) were obtained from the Ocean Drilling Program repository at Lamont-Doherty Earth Observatory. Data from individual samples are listed in Data Repository Tables 15–21.

### Pleistocene Glaciomarine Deposits

#### Core PC-37, Deep Freeze 1979, Latest Pleistocene

Core PC-37 is a piston core taken in the Mertz Trough near Ninnis Glacier that penetrated 4.7 m (Fig. 9). It consists almost entirely of unstratified, poorly sorted, olive-gray gravelly sandy mud (Domack, 1982), interpreted as an ice-contact till. It has a homogeneous massive texture with occasional rock fragments ( $\leq 2$  cm). The sand fraction is dominated by subrounded to angular quartz and feldspar, and grain analysis of a similar core (PC-29) also found significant garnet, kyanite, clinopyroxene, hornblende, opaque, and zircon, mostly with an angular and fractured texture (Domack, 1982). We subsampled sandy matrix in PC-37 between 330 and 390 cm.

Detrital zircons in sample PC-37 are extremely heterogeneous in size and appearance, ranging from coarse, faceted fragments to small, colored round grains. In CL, they are likewise mixed, including internally homogeneous, sector-zoned, and oscillatory-zoned types, although overgrowths are rare. We analyzed 62 grains in this sample (Table DR15), most of which are concordant to within 10%. Almost half (46%) of the grains have Pan-African ages between ca. 460 and 600 Ma (Fig. 10A), with the more dominant peak at ca. 570 Ma. Within these Pan-African age grains, mixture modeling indicates subpopulations at ca. 474 Ma (11% of the 46% total that is Pan-African), 512 Ma (18%), 538 Ma (25%), and 570 Ma (47%). Most of these grains show CL structures and Th/U ratios indicating igneous growth, but some are likely to be metamorphic. The sample also contains scattered Neoproterozoic to Paleoproterozoic grains, including notable groups at ca. 1235 and ca. 2235 Ma. The youngest zircon (3) is a small, round grain that has a  $^{206}\text{Pb}/^{238}\text{U}$  age of  $257 \pm 4$  Ma. The dominant provenance input to this till is clearly a Pan-African-age orogenic source from a combination of magmatic and metamorphic rock types, suggesting that the Ross orogen extends well beyond Victoria Land into Wilkes Land, where Ross-age granites are known from as far west as Cape Webb and Penguin Point (Fanning et al., 2002; Duclaux et al., 2007) and yield Ross-age  $^{40}\text{Ar}/^{39}\text{Ar}$  ages (Di Vincenzo et al., 2007). The till includes Grenville-age and older detritus, but we were unable to differentiate a glacial first-cycle or recycled provenance.

#### Core PC-52, Deep Freeze 1979, Latest Pleistocene

Core PC-52 is a second piston core taken near the shelf edge at Ninnis Bank that penetrated 5.8 m (Fig. 9). It consists of mostly stratified,

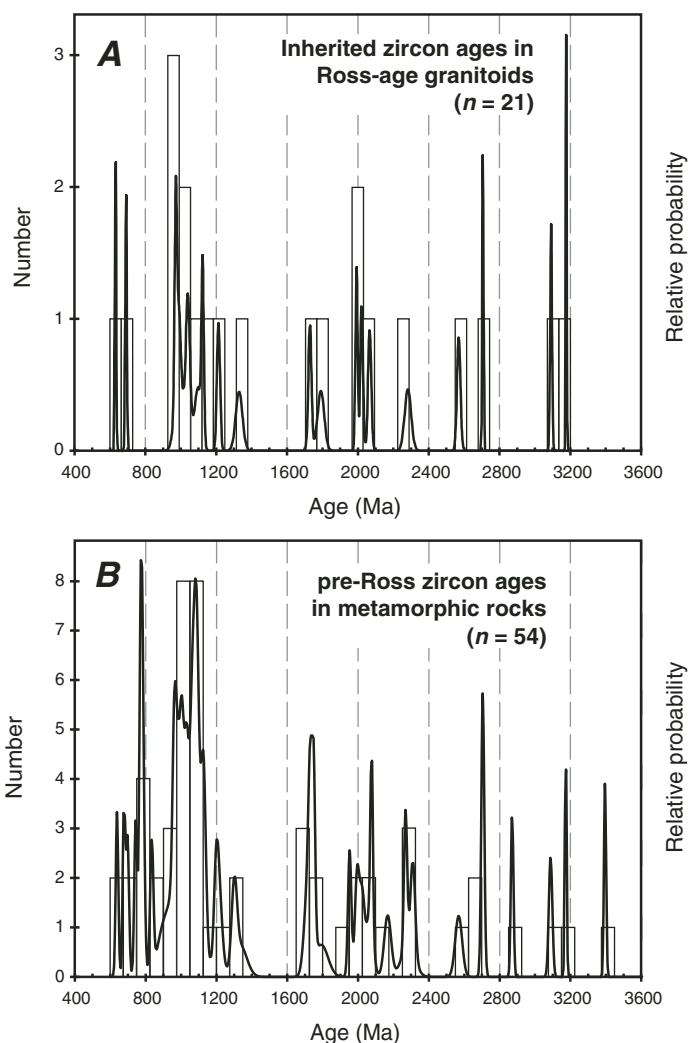


**Figure 8.** Histograms and relative probability distributions of pre-Ross orogen age components in igneous and metamorphic clasts. (A) Ages of inherited zircon >600 Ma in Ross-age granites, obtained in most cases from cores within younger igneous grains. (B) Ages of all zircon analyses older than 600 Ma obtained in metamorphic rocks.

poorly sorted, olive-gray sandy mud with occasional laminations and sand lenses near the top (Domack, 1982), and it is interpreted as a stratified glaciomarine diamicton. Most of the recovered material consists of brown homogeneous gravelly sandy mud with abundant angular to subangular rock chips and fragments. Like PC-37, the sand fraction is quartz and feldspar rich, with significant clinopyroxene, garnet, kyanite, and well-rounded zircon. We subsampled an interval near the top characterized by laminations and sandy intervals between 100 and 160 cm.

Detrital zircons in sample PC-52 are typically coarse yet heterogeneous in appearance, and they generally consist of two types: clear to light-colored prisms and angular fragments, and dark-colored round, elliptical, and subround

grains. In CL, the coarse angular grains typically show broad sector and oscillatory zoning, terminated against the grain edge, whereas the round or prismatic grains show complex internal zonation and narrow overgrowths. We analyzed 60 grains (Table DR16), and most of the areas analyzed are low in common Pb. On a Tera-Wasserburg plot of the total ratios, the resulting analyses are close to or within uncertainty of the concordia curve; one exception (grain 54) contains a high proportion of common Pb and has a  $^{206}\text{Pb}/^{238}\text{U}$  age of  $781 \pm 9$  Ma. Of the whole population, 35 (58%) have Pan-African ages between ca. 535 and 605 Ma, with a prominent peak at ca. 580 Ma (Fig. 10B). Of these, mixture modeling indicates discrete subpopulations at 542 Ma (29%), 581 Ma (55%), and 617 Ma (16%).

The remaining grains are dominantly Neoproterozoic ( $\leq 1300$  Ma), with a few Paleoproterozoic and Archean ages. Unlike early Paleozoic samples of the active Gondwana margin (e.g., Ireland et al., 1998; Goode et al., 2002, 2004), there is no significant Grenville-age contribution. The single youngest grain (57) has an age of  $110 \pm 1$  Ma; this may come from igneous activity associated with incipient rifting between present-day Antarctica and Australia. The detrital zircon ages in this sample indicate a major Pan-African (late Neoproterozoic) provenance, probably derived from glacial erosion of Ross orogen igneous and metamorphic basement that is otherwise unknown from exposure in this part of Wilkes Land. As found in other older sedimentary successions (Goode et al., 2004), the high proportion of ages at ca. 580 Ma, and even older, indicate that Ross orogen magmatism was initiated much earlier than represented by presently exposed plutonic units (commonly in the range of 480–540 Ma).

**Core JPC-11, NBP01-01, Latest Pleistocene**

JPC-11 is a Jumbo piston core that penetrated 24 m of glacial sediments at the edge of the Ninnis Trough (Fig. 9). The upper ~2250 cm consist mostly of thinly layered diatomaceous mud, with occasional pebble-size dropstones interpreted as ice-rafted debris (Leventer et al., 2006). Beginning at ~150 cm from the bottom, there is a marked change from diatomaceous mud to clay-rich structureless diamicton containing increasing proportions of pebble-size clasts in a gray mud matrix. We took a subsample from this core between 2320 and 2380 cm, consisting of gray mud with abundant pebbles and gritty sand matrix. In this interval, the pebbles are mostly small ( $\leq 1$  cm) and angular, and smear slide shows the sand size fraction to consist mostly of subangular to angular colored grains.

Detrital zircons in this sample are extremely heterogeneous, including coarse angular fragments with broad sector or oscillatory-zoned structure in CL, small round colored grains showing multiple CL domains, and rare well-formed prisms with oscillatory-zoned igneous internal structure. We analyzed 60 zircons in sample JPC-11, most of which have concordant or near-concordant ages; some grains with younger ages have low common Pb and so plot close to or within uncertainty of the Tera-Wasserburg concordia curve (Table DR17). Most of the grains (55%) have  $^{206}\text{Pb}/^{238}\text{U}$  ages between ca. 510 and 660 Ma, with a dominant mode at ca. 590 Ma (Fig. 10C). Within the 660–510 Ma range, mixture modeling indicates that there are several subpopulations at ca. 523 (14%), 553 (20%), 587 (33%), 611 (21%), and

**Deep Freeze piston cores**

**N B Palmer piston cores**

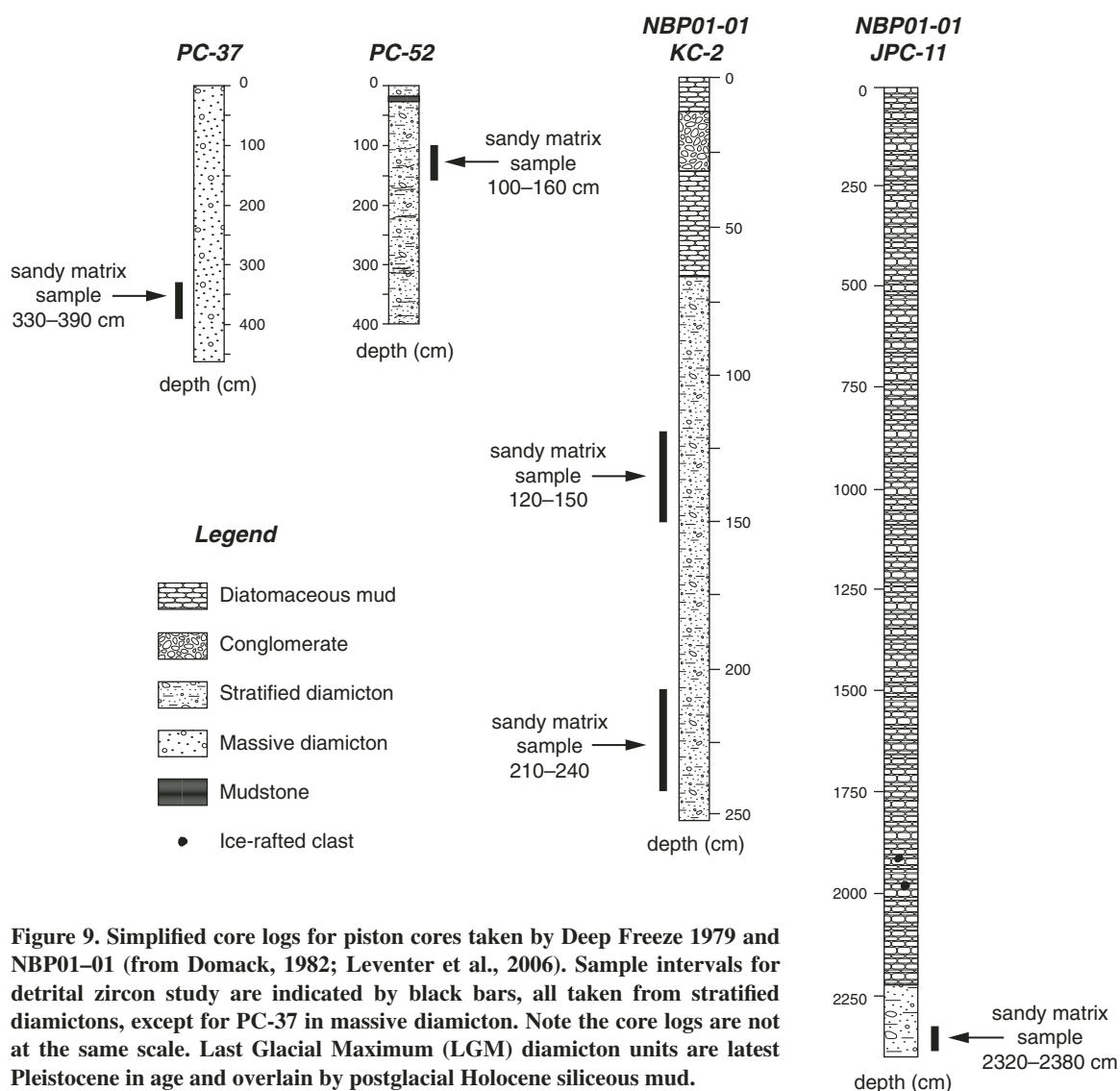


**Figure 9.** Simplified core logs for piston cores taken by Deep Freeze 1979 and NBP01-01 (from Domack, 1982; Leventer et al., 2006). Sample intervals for detrital zircon study are indicated by black bars, all taken from stratified diamictions, except for PC-37 in massive diamiction. Note the core logs are not at the same scale. Last Glacial Maximum (LGM) diamiction units are latest Pleistocene in age and overlain by postglacial Holocene siliceous mud.

647 (12%) Ma. The sample includes grains with a range of Proterozoic and Archean ages, including small but notable peaks at 1200, 1665, and 1905 Ma; the oldest grain (54) has a  $^{207}\text{Pb}/^{206}\text{Pb}$  age of  $3235 \pm 7$  Ma. The single youngest grain has a  $^{206}\text{Pb}/^{238}\text{U}$  age of  $316 \pm 4$  Ma. The sediment sampled by this piston core is dominated by Pan-African ages that we attribute to igneous and metamorphic basement of the Ross orogen. Neoproterozoic contributions from Grenville-age belts are unusually sparse, and there are at least two minor subpopulations of Paleoproterozoic material. The predominant Pan-African ages can be explained either by a broader distribution of the Ross orogen than is generally recognized in this region of Wilkes Land, or by the fact that these glaciogenic deposits contain

recycled components from older sedimentary basins underlying the East Antarctic Ice Sheet. For reasons outlined later herein (see Beacon Supergroup), the latter explanation is less likely.

**Core KC-2, NBP01-01, Latest Pleistocene**

Core KC-2 is a Kasten core that penetrated 2.5 m in the Mertz Depression (Fig. 9). The upper 66 cm consist of bioturbated diatomaceous mud, but the remaining core is olive-gray structureless diamiction (Leventer et al., 2006). It is mostly homogeneous mud with occasional gritty sediment clots, and it contains sparse clasts ( $\leq 1$  cm) of argillite, diamictite, arkose, and red granite, all faceted and striated. Mineral grains in smear slide are mostly angular fragments. We took a subsample of this core in two

places between 120–150 and 210–240 cm, and these were later recombined for detrital zircon separation.

Detrital zircons in sample KC-2 are dominantly rose- and brown-colored grains, showing both round equant and partial to complete terminated prism shapes. Some grains show compound internal growth zonation in CL, but many show only a single type of oscillatory or sector zonation within truncated fragments, formed prior to grain rounding during sedimentary transport. We analyzed 60 grains in this sample (Table DR18), which yielded mostly concordant and near-concordant ages; five of the grains analyzed are  $>10\%$  discordant. Unlike the other late Pleistocene sediment samples, KC-2 contains mostly Paleoproterozoic and Late Archean age

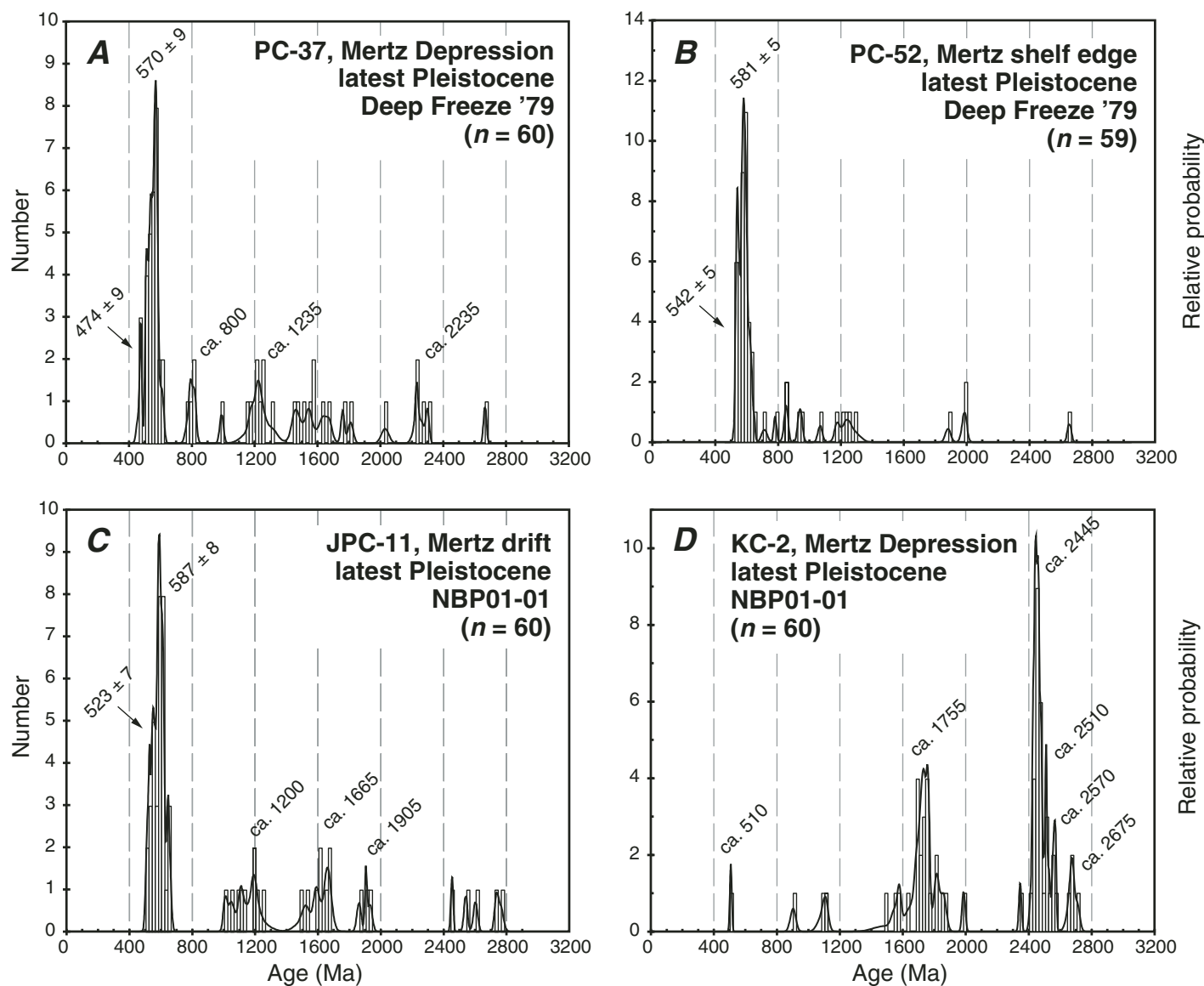


**Figure 10.** Histograms and relative probability distributions of sensitive high-resolution ion microprobe (SHRIMP) U-Pb detrital zircon ages in latest Pleistocene glaciomarine diamictons as sampled by piston core (Table 3). SHRIMP isotopic data are listed in Tables DR15–18 (see text footnote 1).

components (Fig. 10D). The distribution of ages is generally bimodal, with a more prominent Late Archean population and a lesser, but clearly significant, Paleoproterozoic population. The Late Archean grouping has a major age peak at ca. 2440–2460 Ma and minor groups at ca. 2510, 2570, and 2675 Ma. The Paleoproterozoic population has a somewhat diffuse grouping around 1740–1760 Ma with minor peaks at ca. 1820 Ma and just less than 1600 Ma. The single youngest grain (54) has an age of  $508 \pm 6$  Ma, reflecting an extremely subdued Pan-African-age input. Likewise, only three grains have Grenville-orogen ages. Together, these latter results indicate either a different surface

transport direction across only Precambrian terrain compared to other deposits, sedimentary cover over younger source rocks, or both. This sample thus indicates input to the Wilkes Land margin from two major basement provinces of ca. 1.75 and ca. 2.45 Ga age; these ages correlate directly with those of known basement exposures along the nearby Terre Adélie coast (Peucat et al., 1999, 2002; Fanning et al., 2002; Ménot et al., 2005), suggesting that glacial sediment in the Mertz Depression received mostly local input. This sample, unlike others, is not dominated by Ross-age detritus and better reflects the proportions of Precambrian basement known from the region.

### Miocene-Pliocene Continental Rise

#### Site 269, DSDP Leg 28, Miocene-Pliocene

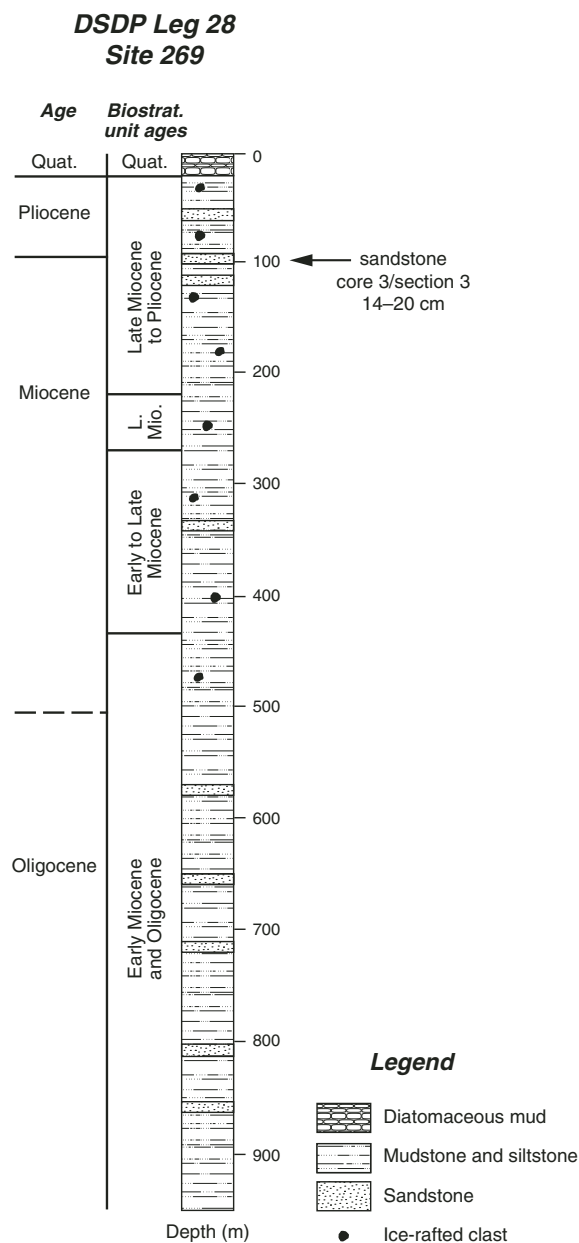
DSDP Site 269 lies at the southeastern margin of the South Indian Abyssal Plain and drilled mostly Neogene turbidites and silts offshore from the Wilkes Land continental slope (Fig. 3). Two holes were drilled (269 and 269A) for a total penetration of 958 m and sediment recovery of 94 m (Hayes et al., 1975). Hole 269A bottomed in Oligocene(?) silty claystone, but the position of the Oligocene-Miocene boundary was not well determined. Sediment in the recovered core consists dominantly of silt and clay, with intermittent fine sandstone and

TABLE 3. SUMMARY OF SEDIMENT SAMPLES USED FOR DETRITAL ZIRCON AGE DATING

Sediment cores	Cruise	Location	Sediment type	Sample interval (cm)	Age
PC-37	Deep Freeze 1979	Mertz Depression	Diamict	330–390	Latest Pleistocene
PC-52A	Deep Freeze 1979	Shelf edge	Diamict	100–160	Latest Pleistocene
JPC-11	NBP01–01	Mertz drift	Diamict	2320–2380	Latest Pleistocene
KC-2	NBP01–01	Mertz Depression	Diamict	120–150, 210–240	Latest Pleistocene
DSDP 269	Deep Sea Drilling Project Leg 28	Wilkes rise	Sandstone	14–20 (core 3)	Miocene-Pliocene
Sedimentary rocks	Area	Location	Rock type	Stratigraphic unit	Age
MN-2-2	Northern Victoria Land	Freyberg Mts.	Subfeldsarenite	Takrouna Fm.	Permian
SP-4	Northern Victoria Land	Rennick Glacier	Lithic feldsarenite	Section Peak Fm.	E-M Jurassic

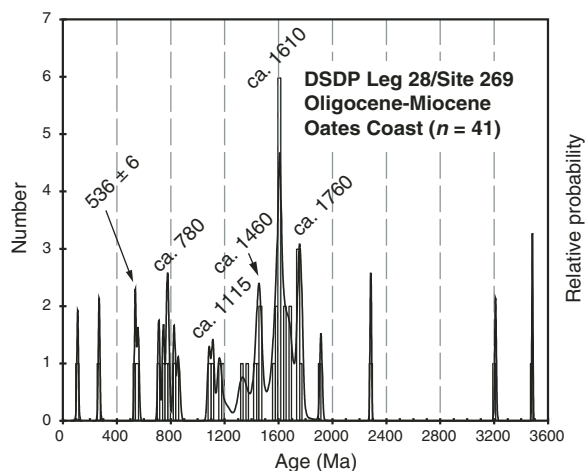
diatomaceous chert, the latter most common in the upper half of the section (Fig. 11). Thin beds of fine sandstone, interpreted as distal turbidites, are present throughout the section, and the intercalated silty clay and clay beds commonly contain ice-rafted clasts. We obtained a sub-sample of silty sandstone from Hole 269/Core3/Section3 at a depth of 97 m below seafloor (Hayes and Frakes, 1975). This sample occurs essentially at the Miocene-Pliocene boundary (ca. 5 Ma), as determined from microflora ages. The sediment in the sampled interval is dominantly olive-gray silty claystone with graded coarse silt and fine sandstone beds ( $\leq 8$  cm). The depositional age, well after onset of Antarctic glaciation, and presence of ice-rafted debris indicate that these continental-rise turbidites have a continental, glacial source.

Detrital zircons from samples from DSDP Site 269 are mostly fine-grained angular fragments, suggesting short-distance transport; many are relatively clear and weakly colored, whereas some appear pitted, frosted, and colored. Internally, they show typical igneous or metamorphic growth zonation in CL, and many display wide oscillatory-zoning or homogeneous rim overgrowths, indicating a young growth stage. Because of a poor yield, we analyzed only 41 zircons from this sample (Table DR19), with the younger zircons ( $\leq 900$  Ma) being more enriched in common Pb and the older zircons ( $>1000$  Ma) yielding mostly concordant analyses. The age distribution is quite mixed; most age periods are represented except mid- to Late Archean (Fig. 12), although many of these come from single analyses that in general do not form distinct age groupings. There is, however, a clustering of analyses in the late Neoproterozoic (ca. 800 Ma) and Mesoproterozoic-Paleoproterozoic (ca. 1600 Ma). We found one late Paleozoic grain (ca. 285 Ma) and two with Pan-African ages, probably from the Ross orogen. The single youngest grain age is  $112 \pm 2$  Ma (grain 14), which probably reflects igneous activity associated with rifting between East Antarctica and Australia. Six grains have ages between 700 and 850 Ma, another six have Grenville-type ages between 900 and 1300 Ma, and four grains



**Figure 11. Simplified core log for sediment core taken at Site 269 by Deep Sea Drilling Project (DSDP) Leg 28 (from Hayes and Frakes, 1975; Anderson, 1999). Most of the recovered core consists of pelagic mudstone intercalated with fine-grained terrigenous siltstone and sandstone interpreted as distal submarine-fan deposits. Sample interval for detrital zircon study is indicated by arrow, taken from fine-grained laminated sandstone dated biostratigraphically to ca. 5 Ma (Miocene-Pliocene boundary).**

**Figure 12. Histograms and relative probability distributions of sensitive high-resolution ion microprobe (SHRIMP) U-Pb detrital zircon ages in Miocene-Pliocene marine sandstone cored at Deep Sea Drilling Project (DSDP) Site 269 (Table 3). SHRIMP isotopic data are listed in Table DR19 (see text footnote 1).**



have Mesoproterozoic ages of 1440–1460 Ma, unique to these samples from the Wilkes margin but observed in older sediments elsewhere (Goode et al., 2002, 2004). The largest representation is from 15 grains that have ages between ca. 1600 and 1750 Ma, with a peak at ca. 1610 Ma. Two grains have ages >3.0 Ga (3 and 21), with the oldest of  $3484 \pm 4$  Ma. Overall, the highly mixed age distribution in sample DSDP Site 269 reflects a heterogeneous source terrain or, more likely, a mixture of first- and second-cycle detritus involving both local and distal sources. Because this sample represents deposition on the continental rise of East Antarctica, it is also possible that it contains contributions from longshore drift that may not be representative of local basement sources.

### Beacon Supergroup Sandstones

As we could not locate existing samples of the Beacon Supergroup from Horn Bluff (Mawson, 1940), we obtained the next closest samples from northern Victoria Land. In the Rennick Glacier area, Beacon strata are divided into three units (Collinson et al., 1986): an unnamed Upper Paleozoic diamictite, the Permian Takrouna Formation, and the Triassic Section Peak Formation. Both of the latter named units rest directly on Lower Paleozoic crystalline basement and consist of terrigenous fluvial sandstone with minor calcareous and noncalcareous mudstone deposited in sandy, braided stream systems. However, the Takrouna and Section Peak units differ markedly in clast composition; the former contains abundant quartz and feldspar grains with sparse lithics, and the latter contains quartz, feldspar, and abundant volcanic rock fragments indicating a calc-alkaline arc source. Paleocurrents in these strata are dominantly to the north and northwest in present-day coordinates, which places their source farther

south in Victoria Land and/or the central Ross orogen. For this study, we obtained two samples of Takrouna and Section Peak sandstone from the U.S. Polar Rock Repository housed at the Byrd Polar Research Center of the Ohio State University; the stratigraphy and petrography of both samples are described in detail by Collinson et al. (1986).

### MN2–2, Takrouna Formation (Permian), Northern Victoria Land

Sandstone sample MN2–2 was collected from a section in the Takrouna Formation near Moawhango Névé and Monte Cassino in the Freyberg Mountains (USPRR ID PRR-04015). The base of the ~200 m section at Monte Cassino rests nonconformably on granitic basement, and another ~100 m of section is exposed at Moawhango Névé. Sample MN2–2 is a medium-grained subfeldsarenite collected from an interval of trough cross-bedded sandstone containing burrows and fossil wood. It is poorly to moderately well sorted, with both clast and matrix support. The sandstone contains angular to subangular grains of quartz (82%), microcline (15%), plagioclase (3%), and muscovite, with traces of biotite, tourmaline, opaque, zircon, and granitic rock fragments (Collinson et al., 1986). Coarse detrital muscovite is bent around framework grains. The grain matrix is presently recrystallized as very fine-grained minerals from the original mud or cement, and it includes minor porosity ( $\leq 5\%$ ).

Detrital zircons in sample MN2–2 are mostly angular to subangular fragments, with less common small subround grains and euhedral prisms. The grains range from colorless to various shades of brown and rosy pink. CL imaging shows that the zircons in this sample come from both igneous and metamorphic sources. Due to the lower abundance of zircon, we analyzed 46 grains in sample MN2–2 (Table DR20); four of

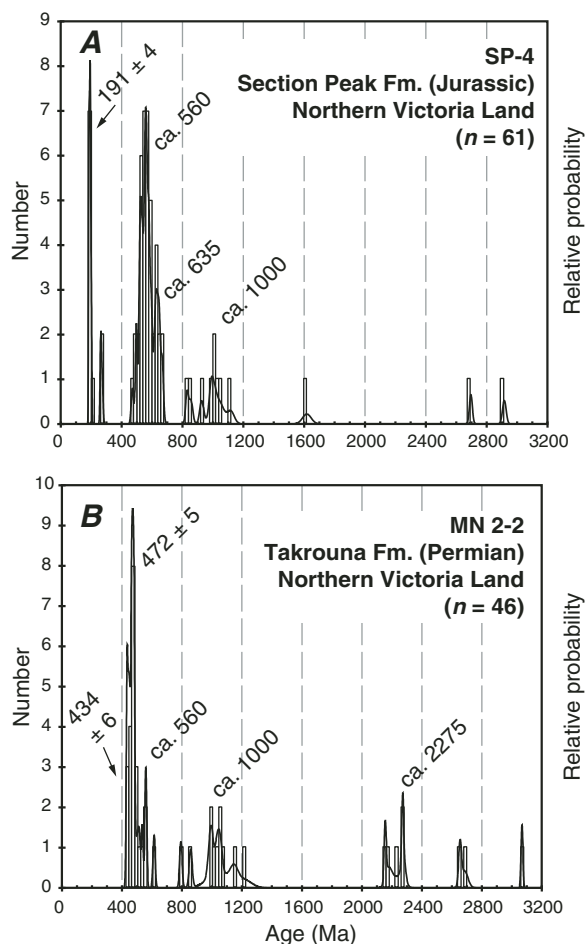
the areas analyzed are significantly enriched in common Pb (grains 9, 21, 36, and 37) and are not considered further. The remaining analyses are mostly concordant to within  $\leq 10\%$ . Detrital zircons in this sample are dominated by Pan-African ages with lesser groupings of Grenville-orogen ages and from the early Paleoproterozoic (Fig. 13B). The Pan-African ages range from ca. 435 to 615 Ma, constituting 50% of the entire sample population; the three youngest grains are  $434 \pm 6$  Ma, but a dominant group of 10 grains has a weighted-mean  $^{206}\text{Pb}/^{238}\text{U}$  age of  $472 \pm 5$  Ma. A younger subordinate component of three grains (10, 14, and 29) has a weighted-mean age of  $434 \pm 6$  Ma. Nine Grenville-age zircons (20%) range from ca. 995 to 1215 Ma, whereas five grains (11%) have early Paleoproterozoic ages between ca. 2150 to 2275 Ma, and there are scattered older Archean grains. The detrital zircon distribution in sample MN2–2 therefore indicates a strongly unimodal late Pan-African-age source, skewed to notably younger ages compared to other samples in this study; this age bias and its cratonic/plutonic sediment composition probably reflect incorporation of material from the uplifted deepest (plutonic) parts of the Ross orogen. Precambrian components are minor but include some early Paleoproterozoic ages.

### SP-4, Section Peak Formation (Triassic), Northern Victoria Land

Sandstone sample SP-4 was collected from the type locality of the formation in the Lichen Hills, ~20 m up from the base of the section overlying granite basement (USPRR ID PRR-04044). Sample SP-4 is a fine- to medium-grained, lithic feldsarenite collected from an interval of cross-bedded sandstone that is locally pebbly and contains abundant fossil wood. The sandstone is poorly sorted, with both clast and matrix support, and it contains very angular to subrounded grains of quartz (68%), microcline (9%), plagioclase (13%), lithic grains (10%), muscovite, biotite, and garnet, with traces of opaque and zircon (Collinson et al., 1986). Lithic grains include volcanic, sedimentary, and granitic rock fragments, in order of decreasing abundance. The matrix is very fine grained and irresolvable optically, presumably mud originally, with close grain packing.

Detrital zircons in sample SP-4 are heterogeneous and include angular fragments, subangular euhedral prisms and faceted grains, and round spherical grains; in color, they range from colorless to yellow, rosy tan, and dark brown. Their appearance in CL section is likewise varied but dominated by oscillatory zoning, with less common sector zonation or homogeneous cores. We analyzed 60 grains in sample SP-4,

**Figure 13. Histograms and relative probability distributions of detrital zircon ages in Beacon Supergroup sandstones collected from northern Victoria Land (Table 3). Sensitive high-resolution ion microprobe (SHRIMP) isotopic data are listed in Tables DR 20–21 (see text footnote 1). Note that the interval sampled in the Section Peak Formation has a maximum depositional age of  $191 \pm 4$  Ma and a minimum depositional age of ca. 176 Ma, the age of the Ferrar dolerite sills that intrude it (see text for discussion); it is therefore late Early Jurassic to Middle Jurassic in age.**



which yielded mainly concordant analyses (Table DR-21). The distribution of zircon ages is dominated by a major subpopulation at ca. 190 Ma (late Early Jurassic) with a broader clustering of analyses between ca. 520 and 620 Ma, peaking at ca. 560 Ma (Fig. 13A). Minor groupings occur at ca. 635 Ma, and a broad population of Grenville-age grains between ca. 950 and 1120 Ma. Two grains (2 and 27) have  $^{206}\text{Pb}/^{238}\text{U}$  ages of ca. 265 Ma (late Early Permian), a constituent not found in sample MN2–2. There is one Paleoproterozoic grain (ca. 1620 Ma) and two Archean grains with ages of ca. 2700 and 2920 Ma. The detritus in this sandstone is dominated by Grenville-age and younger age components, with very little of the Paleoproterozoic and Archean grains found in other samples. Although lacking significant input from older shield rocks, this sediment indicates major input from Pan-African and Early Jurassic magmatic provinces, the latter possibly related to initial stages of Gondwana rifting.

A new constraint on the depositional age of the Section Peak Formation is provided by the ca. 190 Ma zircons. In detail, eight grains (13%)

have  $^{206}\text{Pb}/^{238}\text{U}$  ages between  $185 \pm 2$  and  $201 \pm 3$  Ma, forming an irregular age distribution that can be deconvolved by mixture modeling into a younger group at ca. 187 Ma and an older one at ca. 193 Ma, providing a maximum depositional age. These young zircons are uniformly angular fragments, in many cases, faceted or nearly complete euhedral prisms, indicating they are first-cycle detrital grains; under CL imaging, they show oscillatory zonation indicative of an igneous source. The detrital zircon ages indicate that the depositional age of this interval in the Section Peak Formation is in fact late Early Jurassic to Middle Jurassic, and not Triassic as thought previously (Collinson et al., 1986). The age of these young detrital grains therefore indicates that Section Peak deposition continued almost to the time of Ferrar dolerite sill emplacement (ca. 176 Ma; Fleming et al., 1997).

## DISCUSSION

Glacially transported clasts and detrital mineral suites obtained from Miocene to latest Pleistocene sediments of the eastern Wilkes

Land margin, as well as early Mesozoic fluvial siliciclastics from northern Victoria Land, can be used as proxy tracers for the cratonic geology of a part of East Antarctica. The compositions and ages of these clast and detrital populations help to refine our understanding of East Antarctic geology, evaluate links between Australia and Antarctica, and provide guidance for future remote sensing (mainly airborne geophysics) and drilling operations.

## Clast Compositions and Ages

Lithic clasts recovered by dredge are dominated by low-grade metasedimentary rocks and granitoids, with minor high-grade gneisses and schists. Despite the location of the dredge site off the terminus of Mertz Glacier, where Archean basement is exposed, the relative proportions of the recovered clasts suggest that the eastern Wilkes Land margin is mainly underlain by Paleoproterozoic metasedimentary rocks, and that Archean basement is significantly less abundant. Rock clasts amenable to U-Pb age dating (granitoids and felsic to intermediate gneisses) yielded a bimodal age distribution of 497–584 Ma (11 clasts) and 1722–1741 Ma (3 clasts), respectively. The dominance of ca. 500 Ma granitoid clasts is attributed to the major paleo-ice streams that emerged onto the shelf at Ninnis Glacier (Fig. 3; Domack, 1982), thereby oversampling Ross-age granites relative to the regional geology. Among the 14 dated samples, no Archean clasts were found, although they would be expected in sediment samples farther to the west toward Dibble Ice Tongue. As discussed in the next section, a similar pattern emerges from the detrital zircon age distributions. Together with the known coastal geology, it appears reasonable to infer that much of inland George V Land and Terre Adélie consist of Paleoproterozoic orogenic basement juxtaposed against the western termination of the Ross orogen.

Several of the metamorphic rock clasts discussed earlier contain zircons in the range of 560–580 Ma (Fig. 7), suggesting a young period of metamorphism that slightly predated or was synchronous with early Ross orogen activity. Of additional significance here, however, is the distribution of pre-Ross zircon ages obtained from these six metamorphic rocks as compared to inherited zircons in igneous clasts (Figs. 8A and 8B). Although our data are limited, the metamorphic zircon ages are generally similar to the inherited igneous ages, including groups of ca. 600–800, 900–1300, 1700–2300, and >2600 Ma. Like the inherited zircon components in the Ross-age granitoids, these metamorphic rocks show no evidence

of Mesoproterozoic ages between 1400 and 1600 Ma. Together, these zircon ages suggest that Wilkes Land basement upstream from the Mertz and Ninnis Glaciers includes rock units with discrete Neoproterozoic, Paleoproterozoic, and Archean ages, and that the Ross granitoids sampled from the Wilkes Land glaciomarine deposits likely either intruded or were derived by partial melting of this composite metamorphic basement. Therefore, like the detrital zircon record discussed next, the ages obtained from a large number of metamorphic and igneous clasts can help to establish the age signature of the adjacent ice-covered basement terrain.

### Detrital Zircon Signatures

The samples we studied allow us to assess changing sedimentary provenance on the eastern Wilkes Land margin through time (Fig. 14). The detrital zircon age signatures also record the transition from terrestrial to glaciomarine deposition, corresponding to initiation of the East Antarctic Ice Sheet (ca. 34 Ma; Hambrey and Barrett, 1993; Zachos et al., 1996). Samples of Beacon sandstone, although from farther east in northern Victoria Land and perhaps representative of the Oates coast, indicate that the late Paleozoic and Mesozoic terrestrial landscape was dominated by exposed early Paleozoic orogenic basement. Erosion over time within the early Paleozoic Ross orogen, and deposition of detritus above a Devonian peneplain surface suggest that by middle to late Beacon time, the landscape across much of what is now Victoria Land and Wilkes Land was covered by post-orogenic foreland-basin detritus. A lack of detrital ages older than 1200 Ma indicates that any older basement in this region was likely covered by a broad fluvial-marine basin and therefore unavailable as a sedimentary source. That the eastern Wilkes Land region is underlain principally by Paleoproterozoic and Archean basement is confirmed by the ages of detrital zircons from younger deposits of Miocene and younger age. The glaciofluvial sandstone sample from DSDP Site 269 contains multiple discrete age components between 1100 and 2000 Ma, indicating that growth of the East Antarctic Ice Sheet resulted in significant downcutting into sub-Beacon basement. This sample is dominated by Proterozoic ages, and it may provide the best representation of basement geology in the source area. Its principal age populations of ca. 1610 and ca. 1760 Ma are reflected not only in local basement exposed along the Terre Adélie coast, but also in the younger Pleistocene glaciomarine diamicts. Most of the young glacial deposits are dominated by input from Ross orogen magmatic sources, but one (KC-2) contains a significant

population of ca. 2445 Ma detritus; this age is known from dated on-land geologic units and, although not persistent in all of the late Pleistocene deposits, reflects an important element of Archean age in the eastern Wilkes Land craton.

Like the detrital zircon age distributions, a compilation of all individual zircon ages from the igneous and metamorphic clasts sampled by dredge shows prominent age groups at 0.4–0.6, 0.9–1.2, 1.6–1.9, and 2.4–2.8 Ga (Fig. 14). These age groups, together with the ages of dated units in coastal outcrop, reinforce the age inputs recorded by the detrital zircons. It is apparent from all of these data that the interior region of eastern Wilkes Land, at least in the area bounded by the modern ice-flow catchment (Fig. 2), is dominated by these age components.

### Changing Mesozoic Sources

If we compare the two Beacon samples (Fig. 13), separated by nearly 100 m.y. in depositional age, we find that both are dominated by Pan-African- and Grenville-age components, a common feature in sediments deposited along the Pacific margin of Gondwana. They both contain ca. 560 Ma age populations, but in detail, the Jurassic sandstone is dominated by ca. 560 Ma detritus, whereas the older Permian sample contains mainly ca. 475 Ma detritus. These two age components were likely derived, respectively, from early Ross orogen magmatism followed by late or post-Ross magmatism in the region of northern Victoria Land in the present-day Transantarctic Mountains. The sandstone compositions indicate that the older age group (ca. 560 Ma) represents erosion of a calc-alkaline volcanic-arc source, whereas the younger group (ca. 475 Ma) was derived from more deeply eroded plutonic roots of the magmatic belt. Thus, the composition and age distribution of detrital zircons from these two Beacon Supergroup sandstones confirm a tectonic pattern seen in other detrital records (Goodge et al., 2004)—that of volcanic-arc development in latest Neoproterozoic time (550–580 Ma), followed by growth of a widespread intrusive magmatic belt (470–500 Ma). This is particularly valuable provenance information, given that the Ross orogen-age volcanic province is nearly completely missing from the present-day exposed rock record. The lack of relatively young, post-Ross orogen age components in the younger sandstone (SP-4) may reflect greater postorogenic denudation during formation of the Pangea-wide erosion surface. However, this reassigned Jurassic sandstone contains both Permian and Jurassic igneous components not present in the older sample (MN2-2); the absence of late Early Permian zircons in sample MN2-2 may indicate

that deposition occurred prior to Permian magmatism, thereby constraining deposition of this older formation to before ca. 265 Ma. Neither of the Beacon sandstones contains significant older Precambrian detritus, consistent with earlier interpretations that Beacon deposition was chiefly a result of erosion from Pan-African-age orogenic systems in present-day Africa and East Antarctica (Collinson et al., 1986).

### Comparison of Permian-Triassic and Neogene-Pleistocene Provenance

A comparison of detrital zircon U-Pb ages from samples of the terrestrial Beacon Supergroup and Neogene to latest Pleistocene glaciomarine deposits shows several important differences (Fig. 14): (1) the prominent population at ca. 190 Ma, observed in Beacon sample SP-4, is absent in all of the Neogene-Pleistocene samples; (2) most of the Neogene-Pleistocene deposits contain a strong Pan-African-age population with a concentration between ca. 570 and 590 Ma that is weaker in the Permian sandstone; and (3) both of the Beacon Supergroup sandstone samples lack any significant Paleoproterozoic age components prominent in the younger deposits, and their Archean age components are subdued. Paleocurrent directions from the Section Peak and Takrouna Formations indicate fluvial paleoflow from the interior of Victoria Land toward the present-day Wilkes Land margin (Collinson et al., 1986), although at the time of deposition, East Antarctica and Australia were still united in southern Pangea. Therefore, although the Beacon Supergroup samples we studied may ultimately have a different source compared to the more recent glacial deposits from coastal Wilkes Land, the differences between detrital zircon signatures in the Beacon Supergroup and Neogene-Pleistocene deposits suggest that the latter probably do not contain material simply recycled from interior Paleozoic and early Mesozoic basins. The presence of a few Cretaceous grains (ca. 110 Ma) in the Neogene-Pleistocene deposits, presumably related to Australia-Antarctic breakup, indicates an exposed or glaciated rift-margin source, but the thick succession of Cretaceous and younger fluvial-marine deposits on Early Cretaceous nonmarine basement (Anderson, 1999) may mean that the active rift margin was rapidly covered, hence producing limited detritus.

### Comparison of Proxy and On-Land Wilkes Land Geology

The proxy detrital zircon records show age distributions similar to the known on-land geology of the George V coast and Terre Adélie

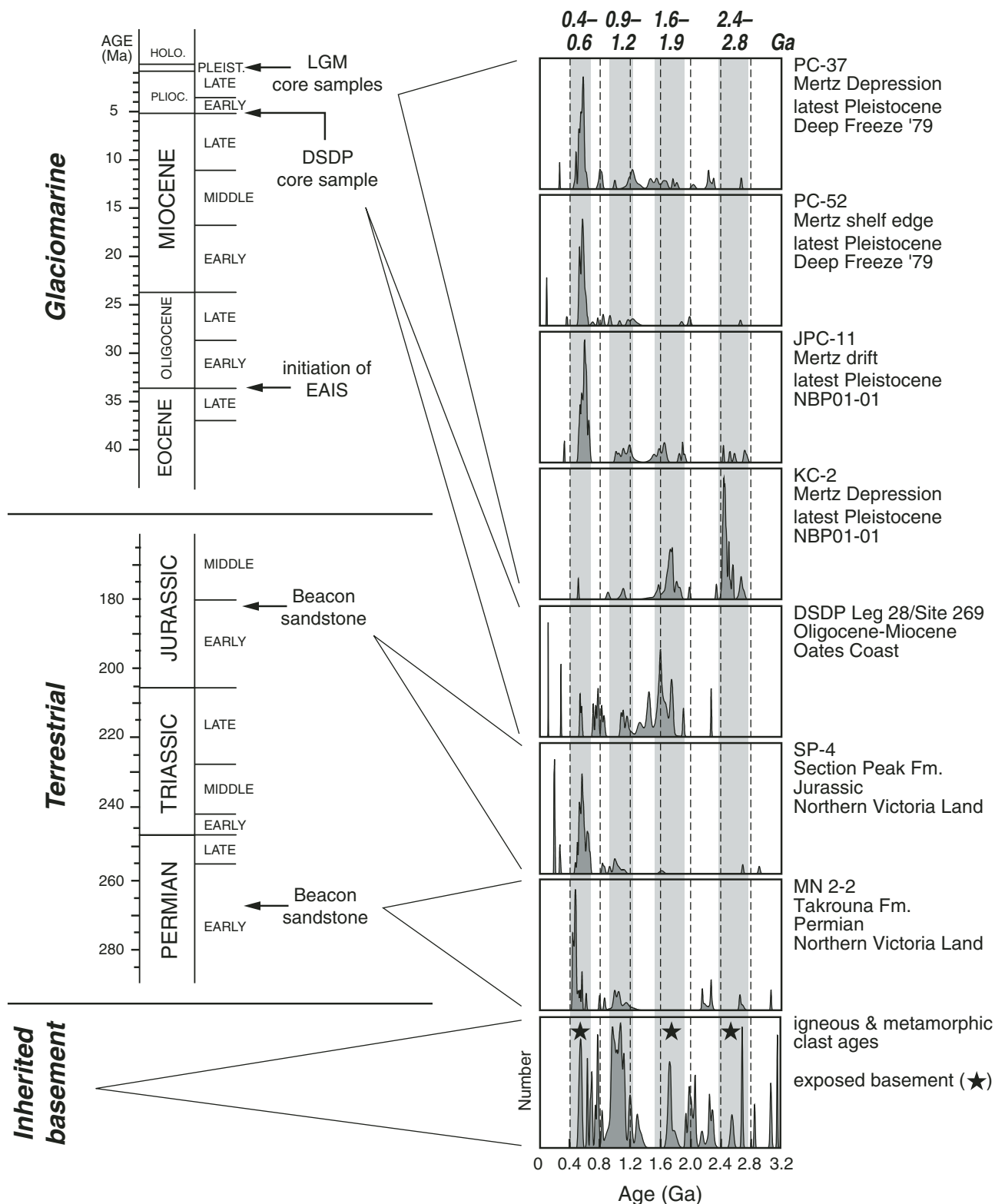


Figure 14. Synoptic summary of detrital zircon relative probability age distributions and histogram of inherited basement age components from this study. Detrital zircon populations are divided into terrestrial sandstones of the Permian-Jurassic Beacon Supergroup and glaciomarine sediments and diamictons of Miocene-Pliocene and latest Pleistocene age. Vertical light-gray bars indicate common age components of ca. 0.4–0.6, 0.9–1.2, 1.6–1.9, and 2.4–2.8 Ga. Plot of inherited basement ages was compiled from all measured sensitive high-resolution ion microprobe (SHRIMP) U-Pb grain ages from igneous and metamorphic clasts; stars indicate general ages of known basement events in Terre Adélie and George V coast area. LGM—Last Glacial Maximum; DSDP—Deep Sea Drilling Project; EAIS—East Antarctic Ice Sheet.

region. All of the ages determined for igneous and metamorphic events in the region are represented in the detrital records, although few of the detrital samples show all of the known events (e.g., JPC-11). There are also no previously unrecognized or exotic age components, although at least one of these (ca. 1.6 Ga felsic volcanism) is known only from large clasts in glacial moraine (Peucat et al., 2002). Thus, the individual glaciogenic detrital records vary in the proportions of different age components, reflecting changes in ice-flow direction, changes in the eroding source over time, reworking of detrital components on the shelf margin, or a combination of all of these. The heterogeneity in the detrital age distribution of these glaciogenic deposits illustrates the need to study multiple samples in such systems in order to recover complete provenance information. Despite this variation, however, the composite detrital age records agree well with the known geology, as highlighted later herein.

Archean grains are present in most of the glaciogenic samples but are most prominent in the KC-2 core, possibly because it was collected near the terminus of Mertz Glacier (Fig. 15), which transects local Archean basement near Cape Denison. This sample confirms the importance of a ca. 2.45 Ga metamorphic event in the region, but it also indicates slightly older activity between ca. 2.5 and 2.7 Ga, a common age for Archean cratons worldwide. Such ages are not known from the local basement, but they may be found as xenocrystic relics with further study.

Sample KC-2 also shows the richest Paleoproterozoic record, with abundant ages between 1600 and 1800 Ma that bracket known ca. 1.7 Ga events (Oliver and Fanning, 1997; Peucat et al., 1999; Ménot et al., 2007). It and sample JPC-11 also contain a few slightly older (1840–1860 Ma) grains that have ages unknown from the local geology, but that may indicate an extension of the Donington granitoid suite into Wilkes Land from South Australia (Fig. 16; Parker et al., 1988; see following). The areally significant granitoid province in Australia does not extend far into East Antarctica, or perhaps was truncated during rifting and separation. The DSDP sample also contains abundant Paleoproterozoic grains, including ca. 1.76 Ga and ca. 1.61 Ga populations; the latter group also is present in lesser amounts in all four of the latest Pleistocene core samples (Fig. 15), and is likely to represent erosion of an igneous source like that of the Gawler Range volcanics (Fanning et al., 1988; Creaser and Fanning, 1993). Although not found in basement outcrop, clasts of rhyolitic volcanic material that match the age and composition of the Gawler Range volcanics in South Australia occur in glacial moraine at

Cap Jules and Port Martin (Peucat et al., 2002). The persistence of this age in most of the Neogene and latest Pleistocene glaciogenic samples indicates that geologic units of the Gawler craton likely extended well into eastern Wilkes Land, particularly a widespread ca. 1600 Ma source terrain, strengthening geologic correlations between East Antarctica and Australia (Figs. 15 and 16; Oliver and Fanning, 1997; Fanning et al., 2002).

Several samples (PC-37, PC-52, and DSDP site 269) together contain a small population of grains between ca. 780 and 800 Ma. These grain ages may record magmatism associated with initial extension associated with early breakup of the Rodinia supercontinent (Harlan et al., 2003). None of these samples, however, contains detrital grains that might be associated with the Cretaceous rifting that led to the separation of Antarctica and Australia.

Granitic rocks from the vicinity of Ninnis Glacier have yielded U-Pb ages of 500–515 Ma (Fanning et al., 2002) and  $^{40}\text{Ar}/^{39}\text{Ar}$  mica cooling ages of ca. 490 Ma (Di Vincenzo et al., 2007). Most of the Neogene and latest Pleistocene glaciogenic samples contain abundant detrital zircon grain ages of ca. 500 Ma that confirm the importance of a Ross orogen source in eastern Wilkes Land. The Mertz Glacier marks a fundamental crustal boundary between the western limit of the Ross orogen and older Precambrian basement (Talarico and Kleinschmidt, 2003), yet Ar cooling ages from the Mertz shear zone indicate that latest movement on this structural zone occurred no later than ca. 1500 Ma (Di Vincenzo et al., 2007); although it is not known how Proterozoic and older basement of eastern Wilkes Land (Terre Adélie craton) was juxtaposed with granitoids of the Ross orogen (Ménot et al., 2005, 2007; Di Vincenzo et al., 2007), it appears the Mertz shear zone is unrelated to Ross displacements. The early record of Ross orogen magmatic activity shown by the latest Pleistocene clast and detrital mineral ages we report is not apparent in geochronology from exposed basement units. Three of the latest Pleistocene core samples (PC-37, PC-52, and JPC-11) are dominated by detrital age peaks between 570 and 580 Ma (Fig. 15), which likely represent input from the Ross magmatic belt; these age populations are matched by three clasts of two-mica granite and granite gneiss (1–8F, 2–1A, 3–7C), which presumably represent samples of plutonic rocks eroded from deep within the Ross magmatic arc. As recorded elsewhere in the Transantarctic Mountains (Goode et al., 2004), these detrital and clast ages demonstrate that Ross orogen magmatism began much earlier (up to ca. 600 Ma) than typically shown by the ages of presently exposed igneous rocks

(mostly 515–490 Ma; Encarnación and Grunow, 1996; Allibone and Wysoczanski, 2002). Protracted continental-margin arc magmatism associated with the Ross orogen should therefore be considered to span more than 100 m.y. between ca. 600 and 500 Ma. The occurrence of granitic clasts with ages of 570–585 Ma, and the corresponding detrital age peaks, may indicate that glacial flow toward Mertz Glacier has eroded an older, more inboard part of the Ross orogen magmatic arc than is otherwise exposed in the modern Transantarctic Mountains.

### Correlation with Elements of the Gawler Craton in Australia

The Gawler craton of southern Australia (Fig. 16; Fanning et al., 1988; Daly et al., 1998; Hand et al., 2007) represents a composite Archean-Proterozoic crustal block that is thought to extend into East Antarctica as part of the broader Mawson Continent (Fanning et al., 1995, 1996). Correlation of geological units and structures, metamorphic patterns, and geochronology suggests a close association of the basement terrains exposed in the Eyre Peninsula and Terre Adélie–George V areas (Fig. 15; Oliver and Fanning, 1997, 2002; Peucat et al., 1999). The Gawler craton is composed of Archean igneous and sedimentary rocks metamorphosed during the ca. 2450 Ma Sleaford orogeny, and then modified by metamorphism and deformation referred to as the ca. 1730–1710 Ma Kimban orogeny; the craton is punctuated by plutonic and volcanic events at ca. 1850, 1680, 1620, and 1590 Ma. In the southern Eyre Peninsula, Archean and Paleoproterozoic metamorphic rocks to the west are juxtaposed with Paleoproterozoic igneous rocks (Donington and Spilsby suites) along the Kalinjala mylonite zone. Monazite cooling ages from the Kalinjala zone suggest that it was active during the latest stages of the Kimban orogeny (Swain et al., 2005). The corresponding elements of the Terre Adélie craton in the area of Terre Adélie and George V coasts include Archean metamorphic rocks of  $\geq 2440$  Ma age juxtaposed to the west against, and partly structurally interleaved with, Paleoproterozoic schists and phyllites (Ménot et al., 2007). Dextral shear fabrics marked by shallow-plunging elongation lineations suggest that the Mertz shear zone forms the eastern boundary of the Archean block, although, as noted earlier, rocks of the adjacent block are covered by Mertz Glacier. The  $^{40}\text{Ar}/^{39}\text{Ar}$  cooling ages suggest that the Mertz shear zone is older than 1500 Ma and therefore does not juxtapose the Archean block with Ross-age granitoids to the east (Di Vincenzo et al., 2007). Similar dextral kinematics and general age correspondence indicate that the

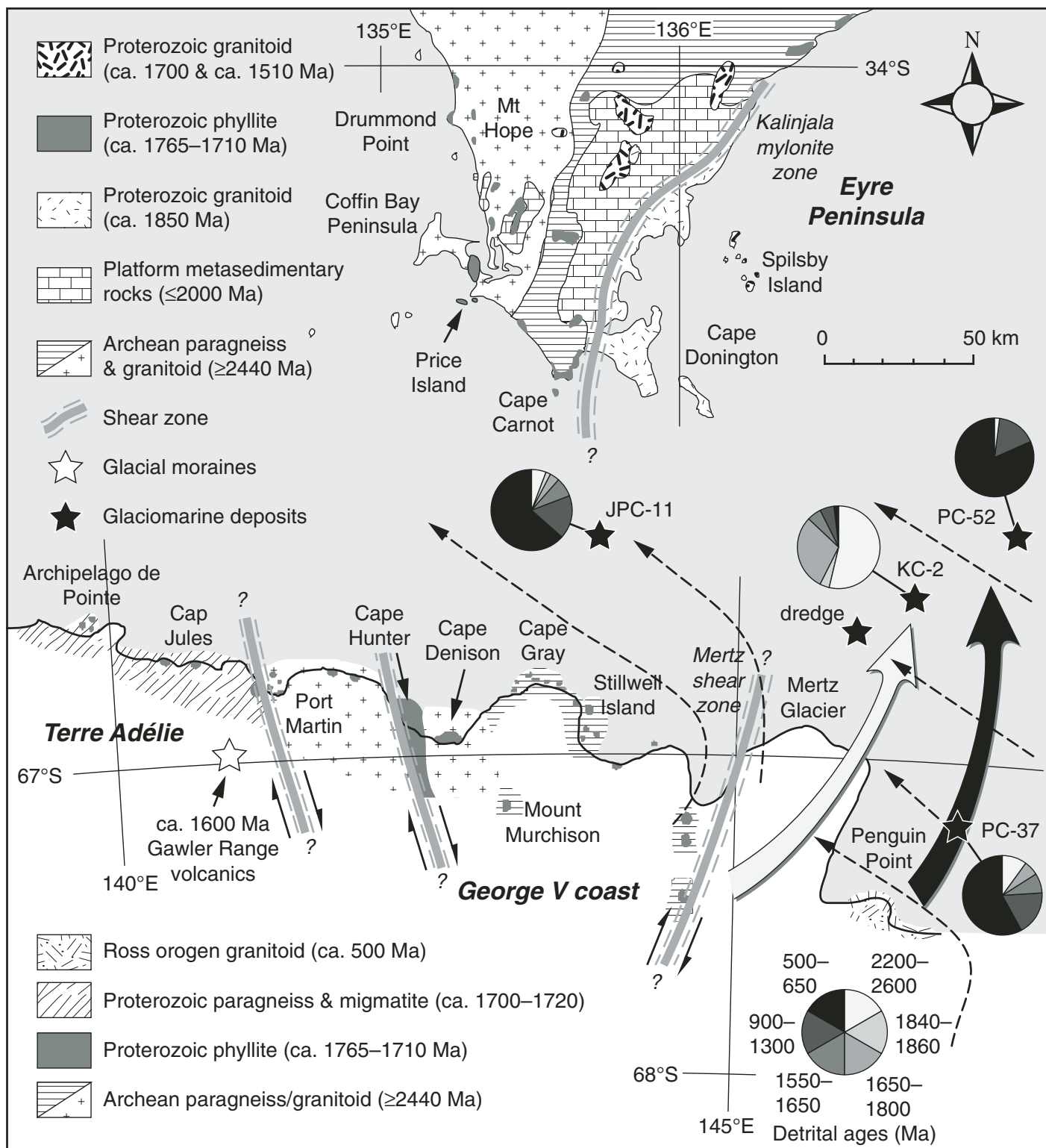
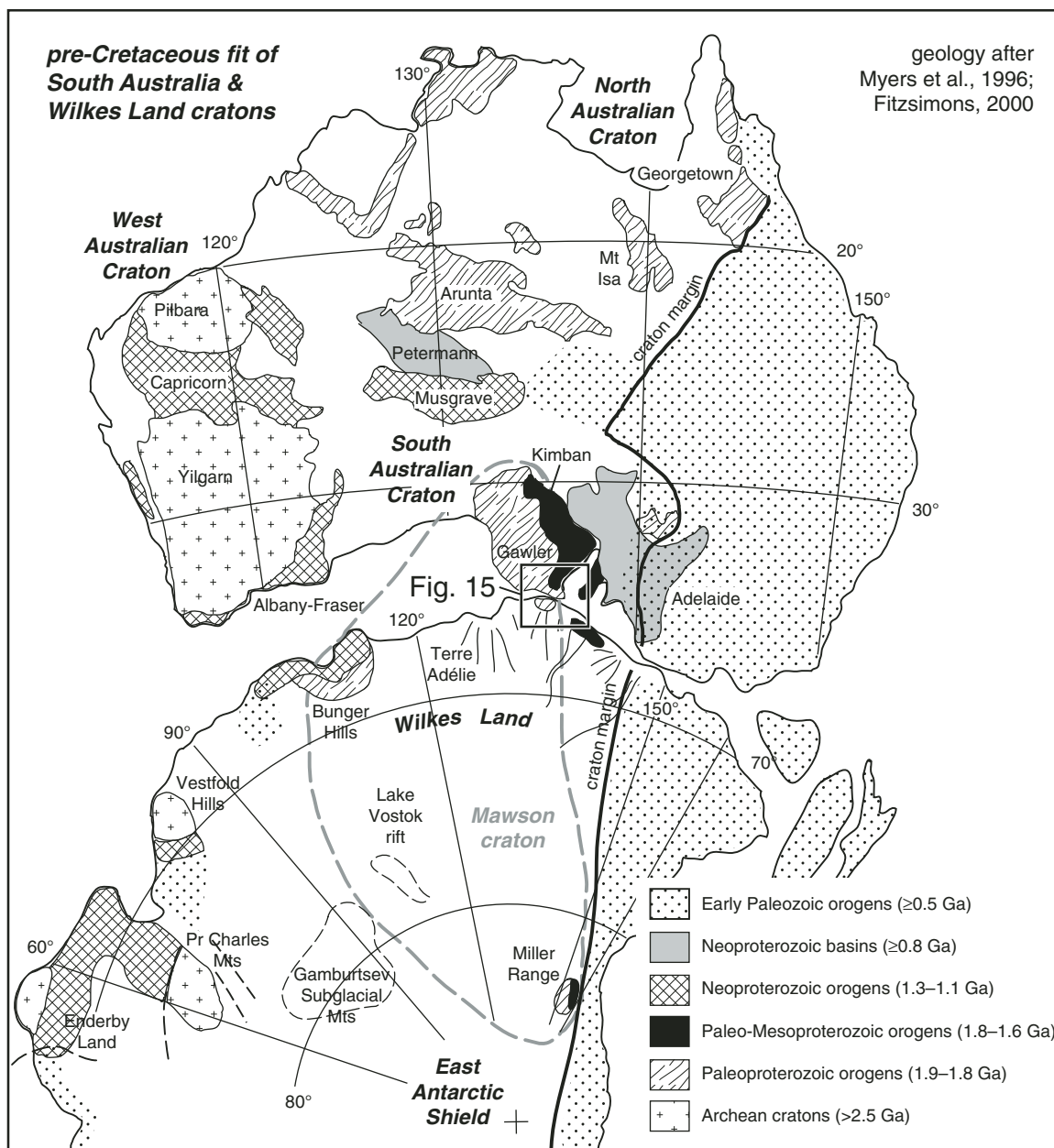


Figure 15. Simplified geology of the Eyre Peninsula region of the southern Gawler craton (South Australia) and the corresponding part of the Wilkes Land margin along the Terre Adélie and George V coasts (after Oliver and Fanning, 1997; Peucat et al., 2002; Duclaux et al., 2007; Ménot et al., 2005, 2007). Reconstructed as in Oliver and Fanning (1997), as shown generally in Figure 1. Dark-gray regions indicate areas of outcrop. Locations of glaciomarine and glacial moraine samples are indicated by stars, as well as Last Glacial Maximum (LGM) ice-flow directions (from Fig. 3; Domack, 1982). Pie diagrams show proportions of detrital zircon age populations within key age intervals (in Ma; see Tables DR 15–18 [see text footnote 1]). Detrital zircon provenance indicates that a sharp geological discontinuity underlies Mertz Glacier, separating Ross orogen–age igneous sources to the east (black arrow) from Archean sources to the west (grey arrow).



**Figure 16.** Geologic correlations between the South Australia and Wilkes Land craton margins. Major basement elements are reconstructed to Cretaceous prerift configuration in East Gondwana (geology modified from Myers et al., 1996; Fitzsimons, 2000). Inset box shows area detailed in Figure 15.

Kalinjala and Mertz shear zones may represent parts of the same Proterozoic translational or transpressional crustal shear system in a restored Gawler–Terre Adélie craton.

The results of our study support the well-established geological correlations between the Gawler and Terre Adélie cratons. The glacial clast and detrital zircon ages confirm the predominance of Archean and Paleoproterozoic geologic elements within the interior on-land region underlain by the modern ice catchment

area. In addition, we recognize minor but distinctive age signatures of ca. 1850 and ca. 1600 Ma not known in present-day Antarctic exposures that may indicate further correlation with known elements of the Gawler craton (Fig. 16).

#### SUMMARY

This study shows the utility of integrating rock and detrital mineral analyses to provide information about the ice-covered cratonic

interior of East Antarctica. Our study used a relatively large suite of glaciogenic materials, including individual crystalline rock clasts and detrital zircon populations, as a proxy for basement in the upstream ice-shed of eastern Wilkes Land. By analyzing materials with different depositional ages, we can also begin to address secular changes in provenance. Nd isotopic analysis of glacially derived sediment deposited along the Antarctic margin can provide average crustal residence ages for basement upstream of

the depositional site (e.g., Roy et al., 2007), yet bulk sediment compositions may not provide sufficiently detailed resolution for identification of hidden individual geologic basement provinces (e.g., Howard et al., 2009). The combination of U-Pb dating of clasts recovered through dredging with detrital zircon geochronology, however, can uniquely provide important compositional and age information about upstream geologic units.

Important findings in this study include the following.

(1) Offshore glaciogenic deposits of Miocene and latest Pleistocene age along the Wilkes Land margin contain clast and matrix materials that can be used as a proxy for inland ice-covered basement. Antarctic glacial-marine sediments contain a record of onshore continental sources, and they can be compared with known geologic provinces to derive a better understanding of the Precambrian basement composition and age distribution. In this study, integration of data from petrologically distinctive individual clasts and large detrital zircon populations provides a good first-order representation of the East Antarctic Shield terrains underlying the eastern Wilkes Land ice sheet.

(2) Igneous and metamorphic rock clasts and detrital zircons from sedimentary units show consistent U-Pb age concentrations of 460–660, 1045–1315, 1545–1815, and 2420–2605 Ma. In detail, there are distinctive age peaks at 545–580, 780, 1110–1220, 1590, 1680, 1760, 2450, and 2665 Ma. Some of these (e.g., ca. 500, ca. 1760, ca. 2450 Ma) are well known from coastal exposures in Antarctica, whereas other age groups are not. The latter group may include clast or grain ages that simply reflect zircon inheritance and recycling, but others may indicate the presence of geologic units not presently exposed. For example, basement of Terre Adélie shows a notable absence of rhyolites like those of the ca. 1590 Ma Gawler Range volcanics of South Australia, yet the glacial-marine detrital record and moraine clasts indicate that this is an important basement element. Likewise, the local geology does not include Grenville-age exposures, but there are abundant Grenville-age zircons in the inherited components of both igneous and metamorphic rock clasts and several of the detrital samples; these may indicate either that Grenville-age basement lies beneath the ice, including rocks with a polygenetic history, or that there are sedimentary and/or metasedimentary rocks containing recycled Grenville-age zircons.

(3) The glaciogenic deposits do not contain significant second-cycle material from Permian–Jurassic cratonic basins. This suggests that Neogene ice flow directly sampled older bedrock.

(4) Basement of the East Antarctic Shield inland from the eastern Wilkes Land margin contains metamorphic rock units with distinctive Paleoproterozoic and Archean ages. Although the clast and detrital zircon populations are dominated by granitoids and metamorphic rocks giving Ross orogen ages, the suite of samples we studied probably undersampled the older basement because sedimentary provenance indicators suggest that paleo-ice flow enriched glacial deposits in the Mertz Glacier area with material derived from the western Ross orogen (Domack, 1982). A contrast in provenance between closely spaced latest Pleistocene cores suggests that there is a sharp crustal boundary underlying Mertz Glacier. Despite this, monzodiorite and charnockitic gneiss clasts with ages of 1720–1740 Ma, as well as common detrital zircon populations in this age range, confirm that basement of this age is an important element in eastern Wilkes Land. These samples correlate in age with ca. 1.7 Ga rocks elsewhere in Wilkes Land and the central Transantarctic Mountains (Goodge and Fanning, 1999; Peucat et al., 1999; Goodge et al., 2001). Together with rocks of this age from the Gawler craton of South Australia, available data show the significance of a greater ca. 1.7 Ga Mawson craton linking present-day East Antarctica with South Australia (Fig. 16).

(5) Ross orogen–age granitoids extend as far west as Mertz Glacier on the coast, and the predominance of a ca. 500 Ma age component in the latest Pleistocene glacial deposits indicates that inland areas of the George V coast may be underlain by extensive Ross orogen granites. Zircon characteristics of the granitoid clasts indicate that they either intruded or were derived by partial melting of composite metamorphic basement. Magmatic rocks of the Ross orogen have been dated previously at 500–515 Ma (Fanning et al., 2002), yet several of our clast samples (1–8F, 2–1A, 3–7C) and the detrital mineral samples indicate that magmatism was initiated as early as 570–585 Ma. The older ages may signify erosion of early Ross orogen granitoids from a more inboard part of the magmatic arc than is otherwise exposed in the modern Transantarctic Mountains.

#### ACKNOWLEDGMENTS

Discussions with John Anderson, Eugene Domack, and Amy Leventer provided significant early inspiration for this project and generous time guiding sample selection. We thank the following individuals and institutions for help in obtaining sample material for this study: (1) Eugene Domack (Hamilton College) and Amy Leventer (Colgate University), co-investigators of the CHAOS cruise of the R/V *Nathaniel B. Palmer* NBP01-01; (2) Matt Curran (Florida State University) and Antarctic Research Facility; (3) Gar Esmay (Lamont-Doherty Earth Observatory and Ocean Drilling Program core repository); and (4) Anne Grunow

(Ohio State University and U.S. Polar Rock Repository). We also thank Jim Collinson for guidance in selecting samples of Beacon Supergroup. This work was supported by an award from the U.S. National Science Foundation (0337858). Clast petrography and geochemical analysis preparations were completed by Diane Curelli and Katie Brosch (both of the University of Minnesota–Duluth); geochemical analysis was completed by Jeff Thole (Macalester College). We thank journal reviewers Eugene Domack and Ian Millar for their helpful comments, and appreciate the many good editorial suggestions by Rob Rainbird.

#### REFERENCES CITED

- Allibone, A., and Wysoczanski, R.J., 2002, Initiation of magmatism during the Cambro-Ordovician Ross orogeny in southern Victoria Land, Antarctica: *Geological Society of America Bulletin*, v. 114, no. 8, p. 1007–1018, doi: 10.1130/0016-7606(2002)114<1007:IOMDTC>2.0.CO;2.
- Allibone, A.H., Cox, S.C., and Smillie, R.W., 1993, Granitoids of the Dry Valleys area, southern Victoria Land: Geochemistry and evolution along the early Palaeozoic Antarctic craton margin: *New Zealand Journal of Geology and Geophysics*, v. 36, p. 299–316.
- Anderson, J.B., 1999, *Antarctic Marine Geology*: Cambridge, UK, Cambridge University Press, 289 p.
- Anderson, J.B., Balshaw, K., Domack, E.W., Kurtz, D., Milam, R., and Wright, R., 1979, Geological survey of East Antarctic continental margin aboard USCGC *Glacier*: *Antarctic Journal of the United States*, v. 14, no. 5, p. 142–144.
- Andrews, J.T., and Matsch, C.L., 1983, *Glacial Marine Sediments and Sedimentation: An Annotated Bibliography*: Norwich, UK, Geo-Abstracts, Bibliography No. 11, 227 p.
- Barker, P.F., Barrett, P.J., Camerlenghi, A., Cooper, A.K., Davey, F.J., Domack, E.W., Escutia, C., Kristoffersen, Y., and O'Brien, P.E., 1998, Ice sheet history from Antarctic continental margin sediments: The ANTOSTRAT approach: *Terra Antarctica*, v. 5, p. 737–760.
- Beaman, R.J., and Harris, P.T., 2003, Seafloor morphology and acoustic facies of the George V Land shelf: *Deep-Sea Research*, v. 50, p. 1343–1355, doi: 10.1016/S0967-0645(03)00071-7.
- Cande, S.C., and Mutter, J.C., 1982, Revised identification of the oldest seafloor spreading anomalies between Australia and Antarctica: *Earth and Planetary Science Letters*, v. 58, p. 151–160, doi: 10.1016/0012-821X(82)90190-X.
- Collinson, J.W., Pennington, D.C., and Kemp, N.R., 1986, Stratigraphy and petrology of Permian and Triassic fluvial deposits in northern Victoria Land, Antarctica: *Geological Investigations in northern Victoria Land, Antarctic Research Series 46*: Washington, D.C., American Geophysical Union, p. 211–242.
- Creaser, R.A., and Fanning, C.M., 1993, A U-Pb zircon study of the Mesoproterozoic Charleston Granite, Gawler craton, South Australia: *Australian Journal of Earth Sciences*, v. 40, no. 6, p. 519, doi: 10.1080/08120099308728101.
- Daly, S.J., Fanning, C.M., and Fairclough, M.C., 1998, Tectonic evolution and exploration potential of the Gawler craton, South Australia: *AGSO Journal of Australian Geology & Geophysics*, v. 17, no. 3, p. 145–168.
- DeConto, R.M., and Pollard, D., 2003, A coupled climate–ice sheet modeling approach to the early Cenozoic history of the Antarctic ice sheet: *Palaeogeography, Palaeoclimatology, Palaeoecology*, v. 198, no. 1–2, p. 39–52, doi: 10.1016/S0031-0182(03)00393-6.
- Di Vincenzo, G., Talarico, F., and Kleinschmidt, G., 2007, An  $^{40}\text{Ar}/^{39}\text{Ar}$  investigation of the Mertz Glacier area (George V Land, Antarctica): implications for the Ross orogen–East Antarctic craton relationship and Gondwana reconstructions: *Precambrian Research*, v. 152, no. 3–4, p. 93–118, doi: 10.1016/j.precamres.2006.10.002.
- Domack, E.W., 1982, Sedimentology of glacial and glacial marine deposits on the George V–Adelie continental shelf, East Antarctica: *Boreas*, v. 11, p. 79–97.

- Duclaux, G., Rolland, Y., Ruffet, G., Ménot, R.P., Guillot, S., Peucat, J.J., Fanning, M., and Pêcher, A., 2007, Superposition of Neoproterozoic and Paleoproterozoic tectonics in the Terre Adélie craton (East Antarctica): Evidence from Th-U-Pb ages on monazite and Ar-Ar ages, *in* Cooper, A., and Raymond, C., eds., *Antarctica: A Keystone in a Changing World—Online Proceedings for the Tenth International Symposium on Antarctic Earth Sciences*: U.S. Geological Survey, Open-File Report 2007-1047, Extended Abstract 072, 4 p.
- Duclaux, G., Rolland, Y., Ruffet, G., Menot, R.P., Guillot, S., Peucat, J.J., Fanning, M., Rey, P., and Pêcher, A., 2008, Superimposed Neoproterozoic and Paleoproterozoic tectonics in the Terre Adélie craton (East Antarctica): evidence from Th/U/Pb ages on monazite and <sup>40</sup>Ar/<sup>39</sup>Ar ages: *Precambrian Research*, v. 167, no. 3–4, p. 316–338, doi: 10.1016/j.precamres.2008.09.009.
- Eittrheim, S.L., Cooper, A.K., and Wannesson, J., 1995, Seismic stratigraphic evidence of ice-sheet advances on the Wilkes Land margin of Antarctica: *Sedimentary Geology*, v. 96, p. 131–156, doi: 10.1016/0037-0738(94)00130-M.
- Encarnación, J., and Grunow, A., 1996, Changing magmatic and tectonic styles along the paleo-Pacific margin of Gondwana and the onset of early Paleozoic magmatism in Antarctica: *Tectonics*, v. 15, no. 6, p. 1325–1341, doi: 10.1029/96TC01484.
- Fanning, C.M., Flint, R.B., Parker, A.J., Ludwig, K.R., and Blissett, A.H., 1988, Refined Proterozoic evolution of the Gawler craton, South Australia, through U-Pb zircon geochronology: *Precambrian Research*, v. 40/41, p. 363–386, doi: 10.1016/0301-9268(88)90076-9.
- Fanning, C.M., Daly, S.J., Bennett, V.C., Menot, R.P., Peucat, J.J., Oliver, R.L., and Monnier, O., 1995, The ‘Mawson block’: Once contiguous Archaean to Proterozoic crust in the East Antarctic Shield and Gawler craton, *in* VII International Symposium on Antarctic Earth Sciences: Siena, Italy, p. 124.
- Fanning, C.M., Moore, D.H., Bennett, V.C., and Daly, S.J., 1996, The ‘Mawson continent’: Archaean to Proterozoic crust in the East Antarctic Shield and Gawler craton, Australia: A cornerstone in Rodinia and Gondwanaland, *in* Kennard, J.M., ed., 13th Australian Geological Convention, Sydney, Geological Society of Australia, v. 41, p. 135.
- Fanning, C.M., Ménot, R.-P., Peucat, J.-J., and Pelletier, A., 2002, A closer examination of the direct links between southern Australia and Terre Adélie and George V Land, Antarctica, *in* Preiss, V.P., ed., *Geoscience 2002: Expanding Horizons*; Abstracts of the 16th Australian Geological Convention: Adelaide, Australia, Geological Society of Australia, p. 224.
- Fitzsimons, I.C.W., 2000, A review of tectonic events in the East Antarctic Shield, and their implications for Gondwana and earlier supercontinents: *Journal of African Earth Sciences*, v. 31, no. 1, p. 3–23, doi: 10.1016/S0899-5362(00)00069-5.
- Fleming, T.H., Heimann, A., Folland, K.A., and Elliot, D.H., 1997, <sup>40</sup>Ar/<sup>39</sup>Ar geochronology of Ferrar Dolerite sills from the Transantarctic Mountains, Antarctica; implications for the age and origin of the Ferrar magmatic province: *Geological Society of America Bulletin*, v. 109, no. 5, p. 533–546, doi: 10.1130/0016-7606(1997)109<0533:AAGOFD>2.3.CO;2.
- Frost, B.R., Barnes, C.G., Collins, W.J., Arculus, R.J., Ellis, D.J., and Frost, C.D., 2001, A geochemical classification for granitic rocks: *Journal of Petrology*, v. 42, no. 11, p. 2033–2048, doi: 10.1093/ptrology/42.11.2033.
- Gapais, D., Pelletier, A., Ménot, R.-P., and Peucat, J.-J., 2008, Paleoproterozoic tectonics in the Terre Adélie craton (East Antarctica): *Precambrian Research*, v. 162, p. 531–539, doi: 10.1016/j.precamres.2007.10.011.
- Goode, J.W., and Fanning, C.M., 1999, 2.5 billion years of punctuated Earth history as recorded in a single rock: *Geology*, v. 27, no. 11, p. 1007–1010, doi: 10.1130/0091-7613(1999)027<1007:BYOPEH>2.3.CO;2.
- Goode, J.W., Fanning, C.M., and Bennett, V.C., 2001, U-Pb evidence of ~1.7 Ga crustal tectonism during the Nimrod orogeny in the Transantarctic Mountains, Antarctica: Implications for Proterozoic plate reconstructions: *Precambrian Research*, v. 112, p. 261–288, doi: 10.1016/S0301-9268(01)00193-0.
- Goode, J.W., Myrow, P., Williams, I.S., and Bowring, S., 2002, Age and provenance of the Beardmore Group, Antarctica: Constraints on Rodinia supercontinent breakup: *The Journal of Geology*, v. 110, p. 393–406, doi: 10.1086/340629.
- Goode, J.W., Williams, I.S., and Myrow, P., 2004, Provenance of Neoproterozoic and lower Paleozoic siliciclastic rocks of the central Ross orogen, Antarctica: Detrital record of rift-, passive- and active-margin sedimentation: *Geological Society of America Bulletin*, v. 116, no. 9, p. 1253–1279, doi: 10.1130/B25347.1.
- Goode, J.W., Vervoort, J.D., Fanning, C.M., Brecke, D.M., Farmer, G.L., Williams, I.S., Myrow, P.M., and DePaolo, D.J., 2008, A positive test of East Antarctica–Laurentia juxtaposition within the Rodinia supercontinent: *Science*, v. 321, p. 235–240, doi: 10.1126/science.1159189.
- Gunn, B.M., 1962, Differentiation in Ferrar dolerites, Antarctica: *New Zealand Journal of Geology and Geophysics*, v. 5, no. 5, p. 820–863.
- Gunn, B.M., 2006, Geochemistry of Igneous Rocks; An eText of Geochemical Data Interpretation, [www.geokem.com/index.html](http://www.geokem.com/index.html). (Accessed November 24, 2009).
- Hambrey, M.J., and Barrett, P.J., 1993, Cenozoic sedimentary and climatic record, Ross Sea region, Antarctica, *in* Kennett, J.P., and Warnke, D.A., eds., *The Antarctic Paleoenvironment: A Perspective on Global Change*, Part 2: Washington, D.C., American Geophysical Union Antarctic Research Series, p. 91–124.
- Hambrey, M.J., Webb, P.-N., Harwood, D.M., and Krissek, L.A., 2003, Neogene glacial record from the Sirius Group of the Shackleton Glacier region, central Transantarctic Mountains, Antarctica: *Geological Society of America Bulletin*, v. 115, no. 8, p. 994–1015, doi: 10.1130/B25183.1.
- Hampton, M.A., Eittrheim, S.L., and Richmond, B.M., 1987, Post-breakup sedimentation on the Wilkes Land margin, Antarctica, *in* Eittrheim, S.L., and Hampton, M.A., eds., *The Antarctic Continental Margin; Geology and Geophysics of Offshore Wilkes Land*: Tulsa, Oklahoma, Circum-Pacific Council for Energy and Mineral Resources, Earth Science Series, v. 5A, p. 75–87.
- Hand, M., Reid, A., and Jagodzinski, L., 2007, Tectonic framework and evolution of the Gawler craton, southern Australia: *Economic Geology and the Bulletin of the Society of Economic Geologists*, v. 102, p. 1377–1395.
- Harlan, S., Heaman, L., LeCheminant, A., and Premo, W., 2003, Gunbarrel mafic magmatic event: A key 780 Ma time marker for Rodinia plate reconstructions: *Geology*, v. 31, no. 12, p. 1053–1056, doi: 10.1130/G19944.1.
- Harley, S.L., and Kelly, N.M., 2007, Ancient Antarctica; the Archaean of the East Antarctic Shield, *in* Van Kranendonk, M.J., Smithies, R.H., and Bennett, V.C., eds., *Earth’s Oldest Rocks: Developments in Precambrian Geology*: Amsterdam, Netherlands, Elsevier, p. 149–186.
- Hayes, D.E., and Frakes, L.A., 1975, General synthesis, Deep Sea Drilling Project Leg 28, *in* Hayes, D.E., Frakes, L.A., et al., eds., *Initial Reports of the Deep Sea Drilling Project*: Washington, D.C., U.S. Government Printing Office, v. 28, p. 919–942.
- Hayes, D.E., Frakes, L.A., et al., 1975, *Initial Reports of the Deep Sea Drilling Project*: Washington, D.C., U.S. Government Printing Office, v. 28, 1017 p.
- Howard, K.E., Hand, M., Barovich, K.M., Reid, A., Wade, B.P., and Belousova, E.A., 2009, Detrital zircon ages: Improving interpretation via Nd and Hf isotopic data: *Chemical Geology*, v. 262, no. 3–4, p. 277–292, doi: 10.1016/j.chemgeo.2009.01.029.
- Ireland, T.R., Flöttmann, T., Fanning, C.M., Gibson, G.M., and Preiss, W.V., 1998, Development of the early Paleozoic Pacific margin of Gondwana from detrital zircon ages across the Delamerian orogen: *Geology*, v. 26, no. 3, p. 243–246, doi: 10.1130/0091-7613(1998)026<0243:DOTPEP>2.3.CO;2.
- Irvine, T.N., and Baragar, W.R.A., 1971, A guide to the chemical classification of the common volcanic rocks: *Canadian Journal of Earth Sciences*, v. 8, p. 523–548.
- Leventer, A., Domack, E., Dunbar, R., Pike, J., Stickley, C., Maddison, E., Brachfeld, S., Manley, P., and McClennen, C., 2006, Marine sediment record from the East Antarctic margin reveals dynamics of ice sheet recession: *GSA Today*, v. 16, no. 12, p. 4–10, doi: 10.1130/GSAT01612A.1.
- Ludwig, K.R., 2001, SQUID 1.02; A User’s Manual: Berkeley Geochronology Center Special Publication 2, 19 p.
- Ludwig, K.R., 2003, User’s Manual for Isoplot/Ex, Version 3.0, A Geochronological Toolkit for Microsoft Excel: Berkeley Geochronology Center Special Publication 4, 70 p.
- Mawson, D., 1940, Sedimentary Rocks, *in* Scientific Reports of the Australasian Antarctic Expedition 1911–14, Ser. A, Geology, Sydney, Government Printing Office, v. 4, p. 347–367.
- McMullen, K., Domack, E., Leventer, A., Olson, C., Dunbar, R.B., and Brachfeld, S., 2006, Glacial morphology and sediment formation in the Mertz Trough, East Antarctica: Palaeogeography, Palaeoclimatology, Palaeoecology, v. 231, no. 1–2, p. 169–180, doi: 10.1016/j.palaeo.2005.08.004.
- Ménot, R.-P., Pelletier, A., Peucat, J.-J., Fanning, C.M., and Oliver, R.L., 1999, Petrological and structural constraints on the amalgamation of the Terre Adélie craton (135°–145°E), East Antarctica, *in* Skinner, D.N.B., ed., 8th International Symposium on Antarctic Earth Sciences: Wellington, New Zealand, Royal Society of New Zealand, p. 208.
- Ménot, R.-P., Pêcher, A., Rolland, Y., Peucat, J.-J., Pelletier, A., Duclaux, G., and Guillot, S., 2005, Structural setting of the Neoproterozoic terranes in the Commonwealth Bay area (143–145°E), Terre Adélie craton, East Antarctica: *Gondwana Research*, v. 8, no. 1, p. 1–9, doi: 10.1016/S1342-937X(05)70258-6.
- Ménot, R.-P., Duclaux, G., Peucat, J.-J., Rolland, Y., Guillot, S., Fanning, M., Bascou, J., Gapais, D., and Pêcher, A., 2007, Geology of the Terre Adélie craton (135–146°E), *in* Cooper, A.K., and Raymond, C.R., eds., *Antarctica: A Keystone in a Changing World—Online Proceedings for the Tenth International Symposium on Antarctic Earth Sciences*: U.S. Geological Survey, Open-File Report 2007–1047, Short Research Paper 048, 5 p.
- Müller, R.D., Gaina, C., and Clarke, S., 2000, Seafloor spreading around Australia, *in* Veevers, J., ed., *Billion-Year Earth History of Australia and Neighbours in Gondwanaland*: Sydney, GEMOC Press, p. 18–28.
- Myers, J.S., Shaw, R.D., and Tyler, I.M., 1996, Tectonic evolution of Proterozoic Australia: *Tectonics*, v. 15, p. 1431–1446, doi: 10.1029/96TC02356.
- Oliver, R.L., and Fanning, C.M., 1997, Australia and Antarctica: Precise correlation of Palaeoproterozoic terranes, *in* Ricci, C.A., ed., *Antarctic Region: Geological Evolution and Processes*: Siena, Terra Antartica Publishers, p. 163–172.
- Oliver, R.L., and Fanning, C.M., 2002, Proterozoic geology east and southeast of Commonwealth Bay, George V Land, Antarctica, and its relationship to that of adjacent Gondwana terranes, *in* Gamble, J.A., Skinner, D.N.B., and Henrys, S., eds., *Antarctica at the Close of a Millennium*: Wellington, New Zealand, Royal Society of New Zealand Bulletin 35, p. 51–58.
- Paces, J.B., and Miller, J.D., 1993, Precise U-Pb ages of Duluth Complex and related mafic intrusions, north-eastern Minnesota: Geochronological insights to physical, petrogenic, paleomagnetic, and tectonomagmatic processes associated with the 1.1 Ga Midcontinent Rift system: *Journal of Geophysical Research*, v. 98, p. 13,997–14,013, doi: 10.1029/93JB01159.
- Parker, A.J., Fanning, C.M., Flint, R.B., Martin, A.R., and Rankin, L.R., 1988, Archaean–Early Proterozoic granitoids, metasediments and mylonites of Southern Eyre peninsula, South Australia: *Geological Society of Australia Field Guide*, v. 2, p. 1–90.
- Pearce, J.A., Harris, N.B.W., and Tindle, A.G., 1984, Trace element discrimination diagrams for the tectonic interpretation of granitic rocks: *Journal of Petrology*, v. 25, no. 4, p. 956–983.
- Peucat, J.J., Ménot, R.P., Monnier, O., and Fanning, C.M., 1999, The Terre Adélie basement in the East-Antarctica Shield: Geological and isotopic evidence for a major 1.7 Ga thermal event; comparison with the Gawler craton in South Australia: *Precambrian Research*, v. 94, p. 205–224, doi: 10.1016/S0301-9268(98)00119-3.

- Peucat, J.J., Capdevila, R., Fanning, C.M., Ménot, R.-P., Pécora, L., and Testut, L., 2002, 1.60 Ga felsic volcanic blocks in the moraines of the Terre Adélie craton, Antarctica: Comparisons with the Gawler Range volcanics, South Australia: *Australian Journal of Earth Sciences*, v. 49, p. 831–845, doi: 10.1046/j.1440-0952.2002.00956.x.
- Roy, M., van de Fliedert, T., Hemming, S.R., and Goldstein, S.L., 2007,  $^{40}\text{Ar}/^{39}\text{Ar}$  ages of hornblende grains and bulk Sm/Nd isotopes of circum-Antarctic glacio-marine sediments; implications for sediment provenance in the Southern Ocean: *Chemical Geology*, v. 244, no. 3–4, p. 507–519, doi: 10.1016/j.chemgeo.2007.07.017.
- Sambridge, M.S., and Compston, W., 1994, Mixture modeling of multi-component data sets with application to ion-probe zircon ages: *Earth and Planetary Science Letters*, v. 128, p. 373–390, doi: 10.1016/0012-821X(94)90157-0.
- Schrum, H., Domack, E., DeSantis, L., Leventer, A., McMullen, K., and Escutia, C., 2004, A glimpse at late Mesozoic to early Tertiary offshore stratigraphy from Wilkes Land, East Antarctica: Results of strategic dredging of the Mertz-Ninnis Trough: *Eos (Transactions of the American Geophysical Union)*, v. 85, no. 47, Fall Meeting Supplement, Abstract PP51E-1359.
- Swain, G.M., Hand, M., Teasdale, J., Rutherford, L., and Clark, C., 2005, Age constraints on terrane-scale shear zones in the Gawler craton, southern Australia: *Precambrian Research*, v. 139, no. 3–4, p. 164–180, doi: 10.1016/j.precamres.2005.06.007.
- Talarico, F., and Kleinschmidt, G., 2003, Structural and metamorphic evolution of the Mertz shear zone (East Antarctic craton, George V Land); implications for Australia/Antarctica correlations and East Antarctic craton/Ross orogen relationships: *Terra Antarctica*, v. 10, no. 3, p. 220–248.
- Tera, F., and Wasserburg, G.J., 1972, U-Th-Pb systematics in three Apollo 14 basalts and the problem of initial Pb in lunar rocks: *Earth and Planetary Science Letters*, v. 14, p. 281–304, doi: 10.1016/0012-821X(72)90128-8.
- Tingey, R.J., 1991, The regional geology of Archaean and Proterozoic rocks in Antarctica, in Tingey, R.J., ed., *The Geology of Antarctica*: Oxford, UK, Clarendon Press, p. 1–73.
- Williams, I.S., 1998, U-Th-Pb geochronology by ion microprobe, in McKibben, M.A., Shanks W.C., III, and Ridley, W.I., eds., *Applications of Microanalytical Techniques to Understanding Mineralizing Processes: Reviews in Economic Geology*, v. 7, p. 1–35.
- Zachos, J.C., Quinn, T.M., and Salamy, K., 1996, High resolution ( $10^4$  yr) deep-sea foraminiferal stable isotope time series: *Paleoceanography*, v. 11, p. 251–266, doi: 10.1029/96PA00571.

MANUSCRIPT RECEIVED 28 APRIL 2008

REVISED MANUSCRIPT RECEIVED 16 OCTOBER 2009

MANUSCRIPT ACCEPTED 27 OCTOBER 2009

Printed in the USA